Characterization of peripheral osmoreceptors

Dissertation zur Erlangung des akademischen Grades des
Doktors der Naturwissenschaften (Dr. rer. nat.)

eingereicht im Fachbereich Biologie, Chemie, Pharmazie
der Freien Universität Berlin

vorgelegt von

Sören Markworth
aus Berlin

Juli 2009

Diese Arbeit wurde vom März 2005 bis Juli 2009 unter der Leitung von Prof. Dr. Gary R. Lewin am Max Delbrück Zentrum für Molekulare Medizin angefertigt.

1.Gutachter: Prof. Dr. Fritz G. Ratjen
2.Gutachter: Prof. Dr. Gary R. Lewin

Disputation am: 09.10.2009

Acknowledgements

First of all, I would like to thank my supervisor Prof. Gary Lewin for giving me the chance to do my PhD in his group. I am grateful for his guidance throughout this work. His support with new ideas, discussions and his never-ending supply of optimism helped me to achieve the aim of my project.
It was a pleasure working in his well-equipped lab and I enjoyed the international atmosphere.

I thank Prof. Dr. Jens Jordan for initiating this interesting project and his support during my study.

I would like to thank Dr. Stefan Lechner for teaching me the whole-cell patch clamp technique and helping me with experimental design and data analysis. His useful advice helped me during my studies and made the work more focussed and therefore easier.

I am grateful for the excellent technical support by Heike Thränhardt, Anke Scheer and Anja Wegner. I would also like to thank Karola Bach for taking care of the animals.

Finally, I would like to thank Dr. Ewan Smith for proof-reading my thesis.

Contents

Abbreviations

AP	Action Potential
CGRP	Calcitonin Gene-Related Peptide
CHO	Chinese Hamster Ovary
CNS	Central Nervous System
DRG	Dorsal Root Ganglia
ECF	Extracellular Fluid
EGFP	Enhanced Green Fluorescence Protein
GDNF	Glial cell line-Derived Neurotrophic Factor
HEK293	Human Embryonic Kidney cells 293
HRP	Horse Radish Peroxidase
HPRT	Hypoxanthine Phosphoribosyltransferase
IB4	Isolectin B4
MAPK	Mitogen-Activated Protein Kinase
MNC	Magnocellular Neurosecretory Cell
MnPO	Median Preoptic Nucleus
nAChR	Nicotinic Acetylcholine Receptor
NGF	Nerve Growth Factor
OVLT	Organum Vasculosum Lamina Terminalis
pERK	Phosphorylated Extracellular Signal Regulated Kinase
PFA	Paraformaldehyde
PVN	Paraventricular Nucleus
RR	Ruthenium Red
RT	Room Temperature
SFO	Subfornical Organ
SON	Supraoptic Nucleus
TRP	Transient Receptor Potential
VP	Vasopressin

List of Figures

1 Introduction

1.1 Body Fluid Homeostasis and Osmolality

The cells of our body are surrounded by a fluid known as extracellular fluid (ECF). It contains substances such as sodium, chloride, potassium, urea, glucose and many others. The osmolality of the ECF is a measure of the concentration of each of these substances and is defined as the number of moles of the chemical compounds in solution per kilogram of solvent. Loss or gain of systemic water or electrolytes results in changes in ECF osmolality which causes water to flow across cell membranes in order to reach an osmotic equilibrium between the cell's cytoplasm and the ECF (Strange 2004). This leads to changes in cell volume and intracellular ionic strength. A hypertonic ECF leads to a decrease of cell volume and hypotonic ECF to an increase in cell volume. Both volume changes can affect the physical integrity of cells and tissues (Steenbergen, Hill et al. 1985). Changes in intracellular osmolality can affect the metabolism and function of individual cells as well as the biological activity of proteins, (Somero 1986). Changes in fluid osmolality of neurons can affect their excitability properties due to altered electrolyte concentrations. For example, in the brain acute changes of ECF osmolality can provoke clinical symptoms from headaches to mental confusion and seizures (Ayus, Varon et al. 2000; Verbalis 2003; Machino and Yoshizawa 2006) and, under extreme conditions, osmotically evoked brain swelling or shrinkage can have traumatic or lethal consequences (Cserr, DePasquale et al. 1987; Gullans and Verbalis 1993). The threat of changes in ECF osmolality is faced by mammals as they interact with their environment and fortunately they have evolved efficient homeostatic mechanisms that strive to maintain ECF osmolality towards a highly stable set-point (Verney 1947; Dunn, Brennan et al. 1973). All mammals maintain a common set-point of ECF osmolality near 300 mOsm/kg whereas some aquatic animals make little effort to osmoregulate and have an ECF

osmolality comparable to their external environment (Dietz, Byrne et al. 1995) (Figure 1).

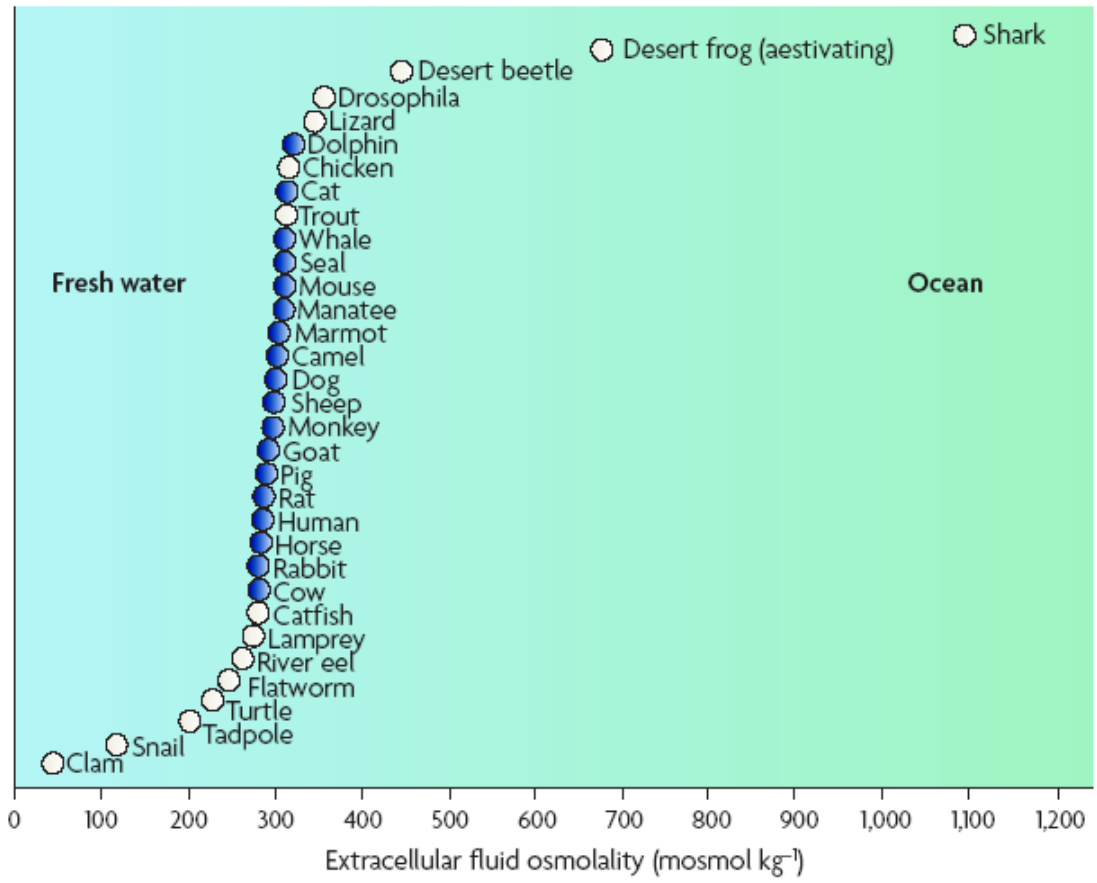

Figure 1: Diagram of the ECF osmolality in animals.
Empty circles mark organisms whose ECF osmolality displays values that can span the full range of environmental osmolalities. Filled circles mark the mammals clustering around an ECF osmolality of 300mOsm/kg (modified from (Bourque 2008)).

The ECF osmolality is a physiological parameter whose stability is aggressively defended by mammals and a highly constant ECF is maintained despite variations in salt and water intake (Darrow and Yannet 1935). Mammals constantly loose water through breathing, urination and sweating due to either external heat or physical activity becoming more and more hyper-osmotic, which triggers behavioral and humoral responses (Figure 2).

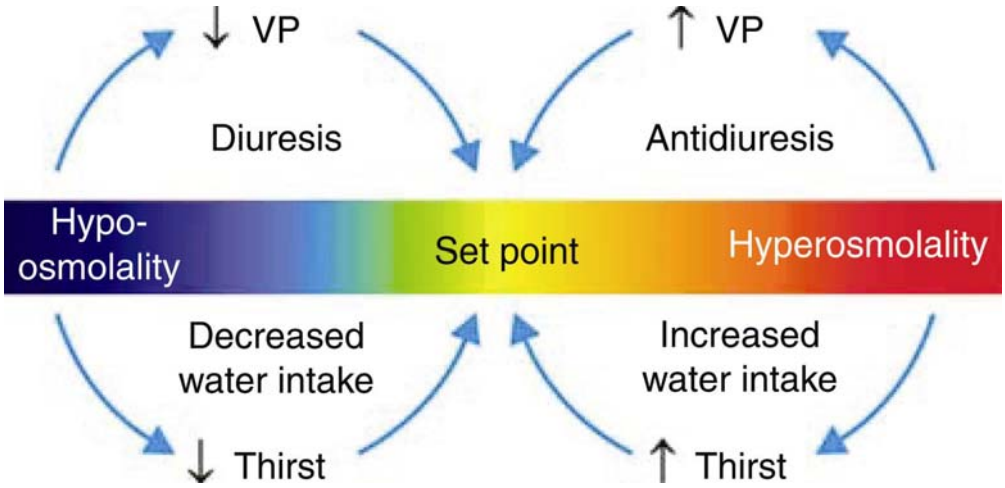

Figure 2: Schema of osmotic regulation.
Systemic water loss leads to systemic hyper-osmolality. This leads to increased levels of vasopressin (VP), antidiuresis and induces thirst. Water intake on the other hand shifts systemic osmolality towards hypo-osmolality, reducing thirst, decreasing VP levels and promoting diuresis (modified from (Sharif-Naeini, Ciura et al. 2008)).

The hypothalamus controls neuroendocrine responses by manipulating the release of natriuretic and antidiuretic hormones such as vasopressin (VP, (Swaab, Pool et al. 1975; Verbalis, Baldwin et al. 1986). VP is synthesized in magnocellular neurosecretory cells (MNCs) of the supraoptic and paraventricular nuclei (SON and PVN) of the hypothalamus (Sofroniew, Weindl et al. 1979; Silverman and Zimmerman 1983). The axons of the MNCs project to the neurohypophysis (posterior pituitary) where hormone secretion into the bloodstream occurs depending on the action potential frequency generated at the MNCs somata (Bicknell 1988). Ingestive behaviors like water and salt intake are controlled by the central nervous system (CNS) through generation of thirst sensation and salt appetite (Andersson 1971; Andersson 1978; Thrasher, Brown et al. 1980; Stricker and Verbalis 1987), while water losses due to breathing and sweating are strongly affected by environmental conditions (Fregly 1967; Greenleaf 1982). A systemic hyper-osmolality induces the sensation of thirst to increase water-intake and stimulates VP release to promote water retention (antidiuresis)

and sodium excretion (natriuresis) by the kidney. An increase of the natriuresis rate has been shown to be produced by infusion of hypertonic solutions in the carotid artery in various mammals including humans (Blaine, Denton et al. 1975; McKinley, Lichardus et al. 1992; Emmeluth, Goetz et al. 1996; Huang, Lee et al. 1996; Andersen, Andersen et al. 2002). This effect is partially mediated by the release of another neurohypophysial peptide, oxytocin, into the bloodstream (Brimble and Dyball 1977). On the other hand hypo-osmolality leads to a reduction in thirst to reduce water-intake and inhibits VP release promoting renal water excretion (diuresis, (Bourque and Oliet 1997)). It has been reported that intravenous infusion of hypotonic solutions reduces the sensation of thirst in dehydrated humans (Maresh, Herrera-Soto et al. 2001). Basal VP levels at rest still partly stimulate renal water reabsorption and therefore the inhibition of VP release due to hypotonic ECF effectively stimulates diuresis (Robertson, Shelton et al. 1976; Claybaugh, Sato et al. 2000). Additionally, hypotonic ECF inhibits the activity of hypothalamic neurosecretory neurons releasing the natriuresis stimulating neuropeptide oxytocin and it is possible that a reduction of central oxytocin levels might increase salt appetite (Brimble and Dyball 1977).

1.2 Osmosensors

The regulation of ECF osmolality is achieved through feedback control which implies the existence of a sensory system capable of detecting changes in osmolality. Gilman's early studies in 1937 (Gilman 1937) showed that cellular dehydration during ECF hyperosmolality is required for thirst sensation. Thirst sensation was evoked in dogs through infusion of hypertonic solutions of membrane-impermeant sodium chloride, but not by infusion of an equivalent osmotic amount of membrane-permeant urea. Gilman concluded that thirst sensation was a consequence of cellular dehydration. Hypertonic solutions containing membrane-impermeant substances lead to water efflux from the cell cytoplasm thereby dehydrating the cell and decreasing its volume

(Gilman and Goodman 1937). At the time it was not known whether thirst sensation occurred as a consequence of a generalized decrease in all cells volume or due to specialized receptor cells being activated by the decrease in volume following changes in ECF osmolality. In 1947 Verney, who conducted similar experiments as Gilman, coined the term osmoreceptor to emphasise their specialized sensory elements and postulated that they consist of “tiny osmometers” and “stretch receptors” with the ability to transmute osmotic stimuli into electrical signals (Verney 1947). Therefore osmoreceptors are defined as neurons with the ability to detect changes in osmolality.

1.3 Central Osmoreceptors

The first description of central osmoreceptors was in 1947 by Verney with his classic experiments on the release of the antidiuretic hormone VP (Verney 1947). Verney showed osmotically triggered VP release using similar experiments with dogs as Gilman 10 years earlier for his study on thirst. The infusion of membrane-impermeant substances such as sodium chloride, sodium sulfate or sucrose in hypertonic concentrations triggered VP release in dogs, whereas an infusion of the similar amount of membrane-permeant urea did not trigger VP release. Despite its permeability across cell membranes, urea only weakly passes through the blood brain barrier (Kleeman, Davson et al. 1962). As urea cannot readily pass the blood brain barrier water flows from the cerebrospinal fluid of the brain into the bloodstream. Thus hypertonic levels of urea in the bloodstream can effectively cause dehydration within the brain compartment. But as such a dehydration of the brain neither effectively triggers thirst sensation nor increased VP secretion it was concluded that central osmoreceptors must be located in regions of the brain lacking a blood brain barrier (McKinley, Denton et al. 1978; Thrasher, Brown et al. 1980). Jewell and Verney established in 1957 that osmoreceptors are located in the anterior region of the

hypothalamus employing experiments featuring intracranial lesions and arterial ligations (Jewell and Verney 1957). Many studies followed reporting that the osmoregulatory reflexes (thirst sensation, VP release) evoked by systemic hypertonicity are inhibited or modulated by lesions in different forebrain structures of the circumventricular organs, which are regions of the brain where the blood brain barrier is weak allowing substances to cross into this region more freely (Buggy and Jonhson 1977; McKinley, Denton et al. 1982; Thrasher, Keil et al. 1982). Supporting these findings it has been shown that injections of hypertonic solutions into the parenchyma of the forebrain triggers or modulates osmoregulatory reflexes (Andersson 1971; Buggy, Hoffman et al. 1979). These and other studies (Bourque, Oliet et al. 1994) suggest the following three brain regions to be responsible for central control of osmoregulation: the subfornical organ (SFO), the median preoptic nucleus (MnPO) and the organum vasculosum lamina terminalis (OVLT). Extracellular electrophysiological experiments on anesthetized rats revealed strong excitation of cells from these regions upon local hypertonic stimulation with pressure injected sodium chloride (Gutman, Ciriello et al. 1988; Honda, Negoro et al. 1990). Moreover whole-cell patch clamp recordings from acutely dissociated OVLT and MnPO neurons demonstrated that these cells respond to hypertonic stimulation with an inward current and increased firing-rate (Richard and Bourque 1994; Ciura and Bourque 2006).

1.4 Peripheral Osmoreceptors

After oral consumption, food passes through the small intestine where solubles and fluid are absorbed from the intestine into vessels of the splanchnic mesentery. From there absorbed fluid and solubles collect into the hepatic portal vein and course through the liver before exiting through the hepatic vein into the vena cava and becoming diluted into the general circulation (Figure 3).

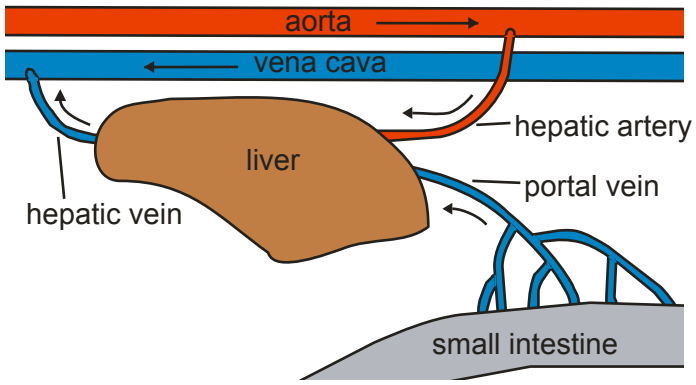

Figure 3: Location of possible early osmosensing tissues.
Schema showing the regions which are passed by ingested food and fluids.Solubles and fluid are absorbed from the small intestine into the hepatic portal vein, course through the liver and exit through the hepatic vein. Arrows mark the blood flow.

The position of the splanchnic mesentery, hepatic portal vein and liver allow them to receive the first absorbed solutes and fluid. Therefore, they represent potentially strategic sites for early detection of systemic osmotic changes resulting from food or fluid intake. In 1968 Haberich observed that the infusion of hypotonic or hypertonic, but not isotonic solutions, into the hepatic portal vein of anesthetized rats increased or decreased the urine volume respectively (Haberich 1968; Haberich 1968). Other studies reported the modulation of VP secretion after hepatic portal vein infusion (Baertschi and Vallet 1981) or intragastral administration of hypo- and hypertonic solutions in rats (Chwalbinska-Moneta 1979; Choi-Kwon and Baertschi 1991). Interestingly, an increase of portal vein blood osmolality can be measured within 7 minutes after intragastric administration of hypertonic sodium chloride solution in rats but systemic osmolality remains unchanged for 15 minutes (Carlson, Beitz et al. 1997). This means peripheral osmoreceptors can detect changes in osmolality due to ingested food or fluid well before central osmoreceptors are able to do so. Therefore, they can induce anticipatory responses through afferent connections to the CNS and buffer the potential impact that consumption related osmotic changes might have.

Indeed, water-drinking causes satiety in thirsty animals and humans before ECF hyperosmolality is fully corrected to normal osmolality levels (Egan, Silk et al. 2003; Stricker and Hoffmann 2007). Dehydration of humans leads to ECF hyperosmolality and increased levels of plasma VP. This is a rapid process, 3 minutes following water-drinking a decrease of the hypertonically elevated VP levels can be detected whereas serum osmolality does not change until 30 minutes after water-drinking (Geelen, Keil et al. 1984). This effect has also been shown in dehydrated sheep (Blair-West, Gibson et al. 1985) and rats (Baertschi and Pence 1995; Huang, Sved et al. 2000). Similarly, intragastric administration of hypertonic sodium chloride solution in rats is reported to stimulate both VP secretion and the sensation of thirst before systemic ECF becomes hyper-osmotic due to the absorbed salt (Carlson, Beitz et al. 1997; Bykowski, Smith et al. 2007; Stricker and Hoffmann 2007). All studies mentioned above deliver indirect evidence for the existence of peripheral osmoreceptors. The important factor is the time frame in which osmoregulation takes place. Osmoregulatory responses are observed shortly after osmotic stimulation at a time point when systemic ECF osmolality is still unchanged and therefore a regulatory response by central osmoreceptors can be excluded. Furthermore, electrophysiological studies revealed that osmotically evoked signaling to the hypothalamo-neurohypophysial system can be abolished by injection of a local anaesthetic into the thoracic region of the spinal cord in rats (Vallet and Baertschi 1982). This region receives innervation fom both the liver and portal vein among other tissues (Berthoud 2004). These results suggest that peripheral osmoreceptors in the liver or portal vein area activate the hypothalamo-neurohypophysial system through a spinal afferent pathway. However, the exact location of peripheral osmoreceptors remains unknown.

1.5 Role of TRP channels in osmosensation

The protein superfamily of transient receptor potential (TRP) channels was named after their founding member TRP which is essential for photoreceptor activity in the fruitfly *drosophila melanogaster* (Cosens and Manning 1969). The fruitfly uses the inositol lipid signaling system for photoreception and a mutation in the *trp*-gene disrupts this process (Minke 1977; Montell, Jones et al. 1985; Montell and Rubin 1989). All members of the TRP-family share six membrane-spanning segments with intracellular N- and C-termini and the ability to augment intracellular calcium levels, either directly via calcium influx through the channels upon activation or organellar calcium release, or indirectly through depolarization of the membrane and secondary calcium entry through voltage dependant calcium channels (Nilius 2007; Damann, Voets et al. 2008). Mammalian TRP-channels are categorized into seven sub-families: TRPC (**c**anonical), TRPV (**v**anilloid), TRPA (**a**nkyrin), TRPM (**m**elastatin), TRPP (**p**olycystin), TRPML (**m**uco**l**ipin) and TRPN (**N**OMPC; **n**o mechanoreceptor potential C). All members are structurally similar to the originally identified *Drosophila* TRP but differ in ion selectivity, modes of activation and physiological functions (Montell 2005). The TRPV subfamily stepped into the spotlight in 1997 with the cloning of the capsaicin receptor TRPV1 (Caterina, Schumacher et al. 1997) and led to subsequent research of its activation by capsaicin, heat and acidic stimuli. Out of the six mammalian TRPV channels three have been suggested to function in the transduction of osmotic stimuli: TRPV1, TRPV2 and TRPV4.

TRPV1 -/- mice have a higher serum osmolality compared to wild type mice (321mOsm/kg and 312mOsm/kg respectively) and both hypertonicity-evoked thirst and VP release were found to be significantly attenuated. Compared to TRPV1 expressed in DRGs, neurons in the supraoptic nucleus (SON) express an N-terminal splice variant of TRPV1 which is osmosensitive but insensitive to capsaicin. Furthermore, electrophysiological studies of both acutely dissociated neurons from the OVLT and acute brain slices of the OVLT from TRPV1 -/- mice revealed that TRPV1 deficient neurons do not show a typical response to hypertonic stimuli (Ciura and Bourque 2006;

Sharif Naeini, Witty et al. 2006). It was concluded that TRPV1 plays some role in hypertonic osmosensation.

The potential role of TRPV2 in osmosensation is based on *in vitro* data only. One study showed that TRPV2 is expressed in murine vascular smooth muscle cells and acutely dissociated aorta cells showed a calcium influx following hypotonic stimulation which could be suppressed by treatment with TRPV2 antisense oligonucleotides (Muraki, Iwata et al. 2003). Additionally, this study showed that TRPV2-transfected chinese hamster ovary (CHO) cells respond with a calcium-influx when hypotonically stimulated. But in the absence of reports of an osmoregulation defect in TRPV2 -/- mice it remains unclear whether TRPV2 is a significant player in osmosensation.

1.6 TRPV4

The first evidence indicating a role of TRPV channels in osmoreception came from experiments performed on the nematode worm *Caenorhabditis elegans* in 1997 (Colbert, Smith et al. 1997). The study demonstrated that worms lacking a functional OSM-9 protein failed to show typical avoidance behaviour when confronted with aversive hypertonicity and odorant stimuli and did not respond to mechanical stimuli applied to the nose. Interestingly, the OSM-9 protein shows homology with the *drosophila* photoreceptor TRP. Further research identified TRPV4 as the vertebrate homolog of OSM-9 being the first mammalian TRPV channel reported to be osmosensitive (Liedtke, Choe et al. 2000; Strotmann, Harteneck et al. 2000). The expression of mammalian TRPV4 in OSM-9 mutant worms could rescue the defects in avoidance of hypertonicity and mechanical stimuli (Liedtke, Tobin et al. 2003). However, defects in avoidance behaviour of aversive odorants could not be rescued by mammalian TRPV4 suggesting that this function differs between invertebrates and vertebrates. Furthermore heterologous expression experiments in CHO and human embryonic kidney 293 cells (HEK293) expressing TRPV4 have shown that these cells gain a *de novo*

ability to respond with reversible calcium signals to hypotonic stimuli and mechanical membrane stretch (Liedtke, Choe et al. 2000; Strotmann, Harteneck et al. 2000).

During the last years TRPV4 -/- mice were generated and many studies either analyzed the involvement of TRPV4 in mechanical pain sensation and hyperalgesia (Alessandri-Haber, Joseph et al. 2005; Alessandri-Haber, Dina et al. 2006), hyperalgesia especially in the viscera (Brierley, Page et al. 2008; Cenac, Altier et al. 2008) or its role in osmosensation. TRPV4 -/- mice are reported to drink less water, are hyperosmolar compared to wild type mice (systemic osmolality of 300 instead of 295mOsm/kg) and when osmotically stimulated their neuroendocrine VP response was diminished (Liedtke and Friedman 2003; Mizuno, Matsumoto et al. 2003) suggesting TRPV4 plays a role in maintenance of systemic tonicity equilibrium.

1.7 Water-drinking in human patients

Patients with orthostatic hypotension due to autonomic neuropathy suffer from a sudden drop in blood pressure when assuming a standing position, usually after a prolonged period of rest. When standing up from a lying position, blood from the thorax flows in the lower extremities compromising venous return which results in decreased cardiac output and subsequently lowering of arterial pressure. Normally this effect triggers vasoconstriction pressing the blood up into the body again but this regulation is defective in such patients. Interestingly, drinking 500ml of water leads to a temporal increase of the blood pressure in these patients within 5 minutes (Jordan, Shannon et al. 1999; Jordan, Shannon et al. 2000; Schroeder, Bush et al. 2002) and also stimulates sympathetic nervous system activity in healthy humans (Jordan, Shannon et al. 2000; Scott, Greenwood et al. 2001). The cause for this reflex is not known. It was speculated that an increase in plasma volume plays a role in this reflex, but further experiments by the same group disproved this hypothesis as intravenous infusion of the same

volume did not show the same effect as water-drinking. A systemic infusion of the ganglionic inhibitor trimetaphan blocks the water-drinking induced increase of blood pressure in orthostatic hypotension patients. Furthermore, water-drinking has been reported to increase blood pressure in paraplegic patients where intact spinal neurons are decoupled from the brain (Tank, Schroeder et al. 2003). These results suggest that the increase in sympathetic nervous system activity is due to a spinal reflex rather then being centrally regulated. As the increase in blood pressure and sympathetic nervous system activity can only be evoked by water, which is hypotonic compared to blood, and not by the same volume of isotonic saline, the trigger for this spinal reflex is probably a change in osmolality which is detected in the peripheral tissue (Lipp, Tank et al. 2005; Raj, Biaggioni et al. 2006).

1.8 Aims

The majority of studies addressing questions about osmoregulation and osmoreception have focused mainly on the involvement of central osmoreceptors, whereas the role of peripheral osmoreception has been given less attention. Although it is known that peripheral osmoreceptors can modulate VP release and thirst sensation as mentioned above (1.4) their exact location remains unknown. Recent studies reported TRPV4 to be able to sense hypotonic changes in osmolality suggesting this channel a potential candidate as peripheral osmosensor.

The first aim of this project was the visualization of osmosensitive neurons in a peripheral tissue that has been postulated to be a potential target for peripheral osmosensation: the liver. A rodent animal model based on immunohistological detection of the activation of the extracellular-signal regulated kinases 1 and 2 (ERK 1/2) was established to quantify the stimulation of hepatic osmosensitive neuronal fibers following water administration of the animal. The role in osmoreception of acutely dissociated sensory DRG neurons from the thoracic region was characterized using Ca^{2+} -imaging and patch clamp techniques. To identify the liver-innervating population of thoracic DRG neurons, a retrograde tracer was injected into the liver of the animals specifically marking liver afferents. Cosequently it was possible to identify liver afferent neurons and to study how these cells react to hypotonicity employing the whole-cell patch clamp technique. An available TRPV4 mutant mouse line was characterized and TRPV4 deficient animals were extensively studied to reveal the functional role of the channel using immonuhistochemical, Ca^{2+} -imaging and whole-cell patch clamp techniques.

2 Material and Methods

2.1 Material

2.1.1 Technical Equipment

Applied Biosystems PRISM 7700 Sequence Detection System
BDK Laminar Flow Hood
Biometra TRIO-Thermoblock PCR machine
Diagnostic Instruments inc., Digitalcamera Model 11.2
Diagnostic Instruments inc., Digitalcamera Model 12.0
EPC-10 amplifier, HEKA
Eppendorf Thermomixer Compact and 5436
EquiBio Easyject Electroporation Apparatus
Forma Scientific -80°C Freezer
Forma Scientific Steri-Cult 200 Incubator
GeneChip Hybridisation Oven
Gilson Minipuls 3 Peristaltic Pump
Harmacia Biotech Ultrospec 1000 Spectrophotometer
Harnischmacher Labortechnik DNA Electrophoresis Chambers
Heidolph Duomax 1030 and Promax 1020 Shakers
Heraeus Biofuge 13
Heraeus Megafuge 1.0
Hereaus Biofuge 15R
Herolab E.A.S.Y 429K Digital Camera
Herolab UVT 2035 Transilluminator 302nm
Ikamag Reo Magnetic Stirrer
Julabo MP and Medingen Waterbaths
Jung Cryostat CM3000
Kreienbaum Wescor VAPRO 5520 Osmometer
Leica DM 5000B Upright Fluorescence Light Microscope

Leica KL 750 Fiber Optic Light Source
Leica MS5 Dissecting Microscope
Mettler Toledo 320 pH Meter
Millipore Multiscreen Resist Vaccum Manifold
Scientific Industries Vortex-Genie 2
Sutter Instrument Patchpipette Puller P-97
Uni Equip Unitherm Hybridization oven 6/12
Visitron Systems, Polychromator Polychrome IV
Zeiss Axiovert 200 Microscope

2.1.2 Analytic Software

7000 System Software 1.2.3, Applied Biosystems
GraphPad Prism 4.0
FitMaster v2.20, HEKA
MetaFluor 7.01, Molecular Devices, Visitron Systems
MetaVue 6.2r6, Universal Imaging Group, Visitron Systems
Microsoft Excel
PatchMaster v.2.11, HEKA
SigmaPlot 9.0, Systat Software
Spot Advanced 4.6, Diagnostic Instruments
Study Size 2.04, CreoStat HB

2.1.3 Chemicals and Reagents

Chemical / Reagent	Company
10 x PCR buffer	Invitrogen Life Technologies
100bp and 1kb ladder	Gibco
2x TaqMan Universal PCR Master Mix	Applied Biosystems
5x First-strand buffer	Invitrogen Life Technologies

5x Second-strand buffer	Invitrogen Life Technologies
Alexa-Fluor 488 Dextranamin MW 3000	Invitrogen Molecular Probes
APES	Sigma-Aldrich
Aqua-Polymount	Polyscience Inc.
Bovine Serum Albumin (BSA)	Invitrogen Life Technologies
CHAPS	Roth
dNTPs (10mM each)	Invitrogen Life Technologies
DTT	Invitrogen Life Technologies
ECL	Amersham Bioscience
EDTA	Sigma
Ethanol	Roth
Fetal calf serum	Biochrom
Fura-2, AM	Invitrogen Molecular Probes
Gelatine	Sigma-Aldrich
Glygogen	Promega Corporation
Gadolinium	Sigma-Aldrich
Glycerol	Sigma
Horse serum	Biochrom
Horse radish peroxidase (HRP)	Sigma-Aldrich
Isopropanol	Roth
Maleic Acid	Fluka
Mannitol	Merck
NBT/BCIP	Roth
Paraformaldehyde	Sigma-Aldrich
poly-L-Ornithin	Sigma
Ketavet 100mg/ml	Pfizer
Laminin	Sigma
Lavamisole	Sigma
Protease inhibitor cocktail	Sigma
RNA*later*	Qiagen
Rompun 2%	Bayer

Ruthenium Red	Sigma-Aldrich
Tissue Tek Cryomold	Sakura
Tissue Tek O.C.T. Compound	Sakura
Triton X-100	Sigma-Aldrich
Trizol	Roth
Tween-20	Pierce Chemical
X-Gal (40mg/ml in DMSO)	Sigma-Aldrich

Further chemicals were obtained from Biomol, Merck, Roth and Sigma-Aldrich

2.1.4 Buffers and Solutions

DRG cell culture:

Buffers / Solutions	**Composition (Company)**
Medium	20% HS (Biochrom) 2mM glutamine (Gibco) 100u penicillin/100µg/ml streptomycin (Gibco) in D-MEM/F12 (Gibco)

Others:

Buffer / Solution	**Composition**
10x TBS	0.5M Tris/HCl pH 7.9 1.5M NaCl
4% PFA	4% paraformaldehyde in PBS pH 7.4
Acetate buffer	Na-acetate 10 mM pH 5
Homogenization buffer	0.1M PBS
Patch clamp buffer - intracellular solution	110 mM KCl 10 mM Na^+ 1 mM $MgCl_2$ 1 mM EGTA

	10 mM HEPES pH7.3, adjusted with KOH
Patch clamp buffer - extracellular solution	110 mM NaCl 1 mM $MgCl_2$ 2 mM $CaCl_2$ 4 mM KCl 4 mM glucose 10 mM HEPES pH 7.4, adjusted with NaOH Mannitol (0mM up to 80mM) was added to adjust the osmolality from 230mOsm/kg up to 310mOsm/kg
PBS	PBS Dulbeco w/o Ca^{2+}, Mg^{2+}
Phosphate buffer	0.1M KH_2PO_4 0.1M Na_2HPO_4 x $2H_2O$
Tail lysis buffer	0.05M Tris (pH8) 0.1M EDTA (pH8) 0.1M NaCl 1% SDS
TCA	20% Trichloracetic Acid

2.1.5 Antibodies

Primary Antibody	Company
Anti-CGRP	Acris Antibodies
Anti-ERK	Cell Signaling
IB4-488	Invitrogen Molecular Probes
IB4-568	Invitrogen Molecular Probes
Anti-pERK	Cell Signaling
Anti-PGP9.5	UltraClone Ltd
Anti-TRPV4	Abcam
Anti-TRPV4	Alomone Biolabs

Secondary Antibody	Company
Alexa-Flour 488	Invitrogen Molecular Probes
Alexa-Fluor 568	Invitrogen Molecular Probes
Alexa-Fluor 647	Invitrogen Molecular Probes
Cy-2	Jackson ImmunoReaserch
Cy-3	Jackson ImmunoResearch

2.1.6 Enzymes

Enzyme	Company
Collagenase TypeIV	Gibco
DNase I (RQ1 RNase free DNase)	Promega
DNAse I	Qiagen
Proteinase K	Roth
Restrictionendonucleases	Amersham, Roche
RNaseA (10mg/ml)	Qiagen
RNaseOUT™	Invitrogen Life Technologies
Superscript II™ reverse transcriptase	Invitrogen Life Technologies

T4 DNA polymerase	Invitrogen Life Technologies
T4-DNA ligase	Promega
T4-DNA ligase	Invitrogen Life Technologies
Taq-DNA polymerase	Gibco
Trypsin	Gibco

2.1.7 Kits

Kit	**Company**
QiaEx Gel Extraction Kit	Qiagen
RNeasy mini kit	Qiagen
RNA transcript labelling kit	Enzo
SuperScript II Reverse Transcriptase	Invitrogen

2.1.8 Primer

Gene	**Company**	**Sequence**
ß-actin	Tib MolBio	aaggccaaccgtgaaaagat gtggtacgaccagaggcatac
Cyclophilin D	Tib MolBio	atggtgaaaaacctgccaaa catcctcagggaagtctgga
HPRT1	Tib MolBio	tcctcctcagaccgctttt cctggttcatcatcgctaatc
TRPV4	Tib MolBio	ccaccccagtgacaacaag ggagctttggggctctgt

2.1.9 Consumables

Product	Company
15ml and 50ml tubes	Falcon, Greiner
Application cannula	Heiland
borosilicate glass capillaries	Hilgenberg, Malsfeld
Cell culture dishes	Falcon
Centricon	Millipore
Coverslips	Roth
Dissection Forceps	FST
Dissection Scissors, Spring Scissors	FST
Eppendorf tubes	Eppendorf
Micro spin columns	Amersham
MicroAmp Optical 96 well reaction plate	Applied Biosystems
MicroAmp Optical 96 well adhesive film	Applied Biosystems
Pipettes	Eppendorf
Quartz cuvettes	Roth
Sterile filters	Nalgene, Millipore
Suturing Needle 16MM	smi
Syringe Needles	Sterican
Syringes (1ml, 5ml, 10ml)	Braun
Whatman filters	Schleicher & Schuell

2.1.10 Animals

C57BL/6N mice were obtained from Charles River Breeding Laboratory, Inc., Wilmington, Massachusetts and kept in the animal house of the MDC until they were used for experiments.

TRPV4$^{-/-}$ mice were obtained from Makoto Suzuki and Masashi Imai, Department of Pharmacology, Jichi Medical School, 3311-1 Yakushiji, Minamikawachi, Tochigi 329-0498, Japan. The mice were kept in the animal house of the MDC until they were used for experiments.

Transgenic α3nAChR-EGFP-mice were bought from GenSat and are a kind gift of Dr. Ines Ibanez-Thallon (MDC, Berlin-Buch).

2.2 Methods

2.2.1 Molecular biology

Standard methods were performed according to Sambrock et al. (1989) and Asubel et al. (1997).

Isolation of genomic DNA from mouse-tail biopsy

About half a centimetre of the tail tips were obtained from adult mice. To digest the tail it was incubated in 700µl Tail lysis buffer containing ProteinaseK (15mg/ml) overnight at 55°C in a shaker (850rpm). The reaction tube was cooled on ice for 10min. To precipitate proteins 300µl NaCl (6M) solution was added, the mixture was briefly vortexed and incubated for 30 min on ice before spinning down the samples in an Eppendorf centrifuge (10'/15,000 rpm) at 4˚C. One millilitre of the supernatant was transferred into a new reaction tube, after adding RNaseA (10mg/ml) the suspension was incubated for 15min at 37°C in a shaker. DNA was precipitated with 1ml Isopropanol and centrifuged at 14,000 rpm at 4°C in an Eppendorf centrifuge. The pellet was washed with 1ml 70% ethanol (cold) and centrifuged at 10'/13,000 rpm at 4˚C for 20min. The dry pellet was resuspended in 50µl 1xTE-buffer. Yields up to 1.5µg genomic DNA are usually obtained with this procedure.

Restriction digest

5-10µg of genomic mouse-tail DNA were used for a ScaI (5U/µg DNA) digestion overnight at 37°C. DNA restriction fragments were separated by gel electrophoresis using a 0.7% agarose gel.

PCR (for TRPV4 genotyping)

For genotyping TRPV4$^{-/-}$ mice the following protocol was used:

1µl genomic tail DNA

2µl 10 x PCR buffer

1µl $MgCl_2$

0.4µl dNTPs (10mM)

0.2µl each 50µM primer (+allel Exon4 f/r, -allel NEO f/r)

0.2µl Taq polymerase.

ad 20µl H_20

PCR cycling:

Initial denaturation:	94°C	7min
Annealing:	60°C	35sec
Extension:	72°C	2min
Denaturation:	94°C	30sec
Annealing:	60°C	35sec
Extension:	72°C	2min
Cycles:	40	
Final extension:	72°C	5min
Storage:	4°C	

PCR reactions using Taq DNA-polymerases

DNA was amplified by PCR using a reaction volume of 30µl:

1.0µl template

3.0µl 10 x PCR buffer

0.9µl $MgSO_4$

1.0µl dNTPs (10mM)

1.0µl primer-mix (1µl primer3' + 1µl primer5' + 8µl water)

22.9µl H_20

0.2µl Taq DNA polymerase.

PCR cycling:

Initial denaturation:	94°C	2-5min
Denaturation:	94°C	30–60sec
Annealing:	55 – 60°C	30–60sec
Extension:	72°C	30–60sec
Cycles:	25–35	

Final extension:	72°C	2-6min
Storage:	4°C	

PCR products were loaded to an agarose gel, bands of the expected size were gel-extracted and where required cloned into the TA-cloning vector pGEM-T Easy, in accordance to the manufacturer's instructions. PCR fragments were analyzed by restriction digest and/or sequencing.

2.2.2 Quantitative Real Time PCR

Whole DRGs

DRGs of the regions of interest were dissected out and immediately put into eppendorf tubes at 4°C (on ice) filled with the RNA-stabilizing reagent RNA*later*. Lysis of cells, isolation and cleaning of total RNA was performed in accordance to the manufacturer's protocol (RNeasy mini kit, Qiagen). For the first strand cDNA synthesis the following protocol (SuperScript II Reverse Transcriptase, Invitrogen) was used:

1µl random hexamer primers
2µg total RNA
1µg dNTPs (10mM each)
ad 12µl destilled water

The mixture was heated to 65°C for 5 min and quickly chilled on ice. The content was collected by brief centrifugation and the following components were added:

4µl 5x first-strand buffer
2µl 0.1M DTT
1µl RNaseOUT^{TM} (40U/µl)

The contents were gently mixed and incubated at RT for 2min. One microlitre Superscript II^{TM} reverse transcriptase was added and the reverse transcription reaction was performed at 42°C for 50min. The reaction was terminated by heat inactivation of the enzyme at 70°C for 15min. If not used immediately the cDNA was stored at -80°C.

2xTaqMan Universal PCR Master Mix (Applied Biosystems) was used for quantitative Real Time PCR amplification reactions in accordance with the manufacturer's instructions:

1.0µl cDNA
0.8µl primer-mix (1µl primer3' + 1µl primer5' + 8µl water)
0.4µl probe
17.8µl water
20.0µl TaqMan Master Mix

The solutions were then transfered to MicroAmp Optical 96 well reaction plates. All reactions were carried out in duplicates (2 x 20µl).

Single Cells

For collection of single cells, a coverslip with cultured DRG neurons was placed in the recording chamber of a patch clamp setup. A patch-pipette with a tip-diameter of 25-35µm was filled with 5-10 µl lysis-buffer (100µl contain 20µl 5x First-Strand Buffer, 5U/ml RNase-inhibitor (12,5µl) and 67,5µl water). The pipette was carefully placed on top of the cellbody and cells were collected by applying negative pressure. For cell lysis the pipette was put into liquid nitrogen for 5s and the solution containing free RNA was collected in eppendorf tubes on dry ice. This solution (around 7µl) was directly used as template for cDNA synthesis.

Real-Time PCR protocol

The MicroAmp Optical 96 well reaction plate was placed into a PRISM 7700 Sequence Detection System machine (Applied Biosystems) and the following program was used:

prewarming:	50°C	2min
initial denaturation:	95°C	10min
denaturation:	95°C	15s
extension:	60°C	1min
cycles:	50 - 60	

The amplification threshold cycles of TRPV4 was compared to threshold cycles of the housekeeping genes HPRT, Cyclophilin D and ß-Actin. Real Time PCR reactions were analyzed using the 7000 System Software 1.2.3 program (Applied Biosystems).

2.2.3 Cell culture

Cultivation of sensory neurons

Mouse DRGs were dissected and collected in a 1.5ml tube in PBS on ice. DRGs were washed once with PBS before incubation with 10µl Collagenase TypeIV in 1ml PBS at 37°C for 30 min. DRGs were briefly centrifuged (170 x g), the supernatant removed and DRGs incubated with 100µl 0.5% Typsin in 1ml PBS at 37°C for 30 min. Digested DRGs were washed with growth medium, triturated using fire-polished Pasteur pipettes to dissociate them into single cells and plated in a droplet of growth medium on a glass coverslip (about 150-200µl of cell suspension per coverslip) precoated with poly-L-lysin (20µg/cm², Sigma-Aldrich) and laminin (4µg/cm², Invitrogen). To allow neurones to adhere, coverslips were kept for 3-4 hours at 37°C in a humidified (5%) incubator before being flooded with fresh growth medium. Cells were grown for 24h at 37°C in a Steri-Cult 200 incubator.

2.2.4 Immunohistochemistry

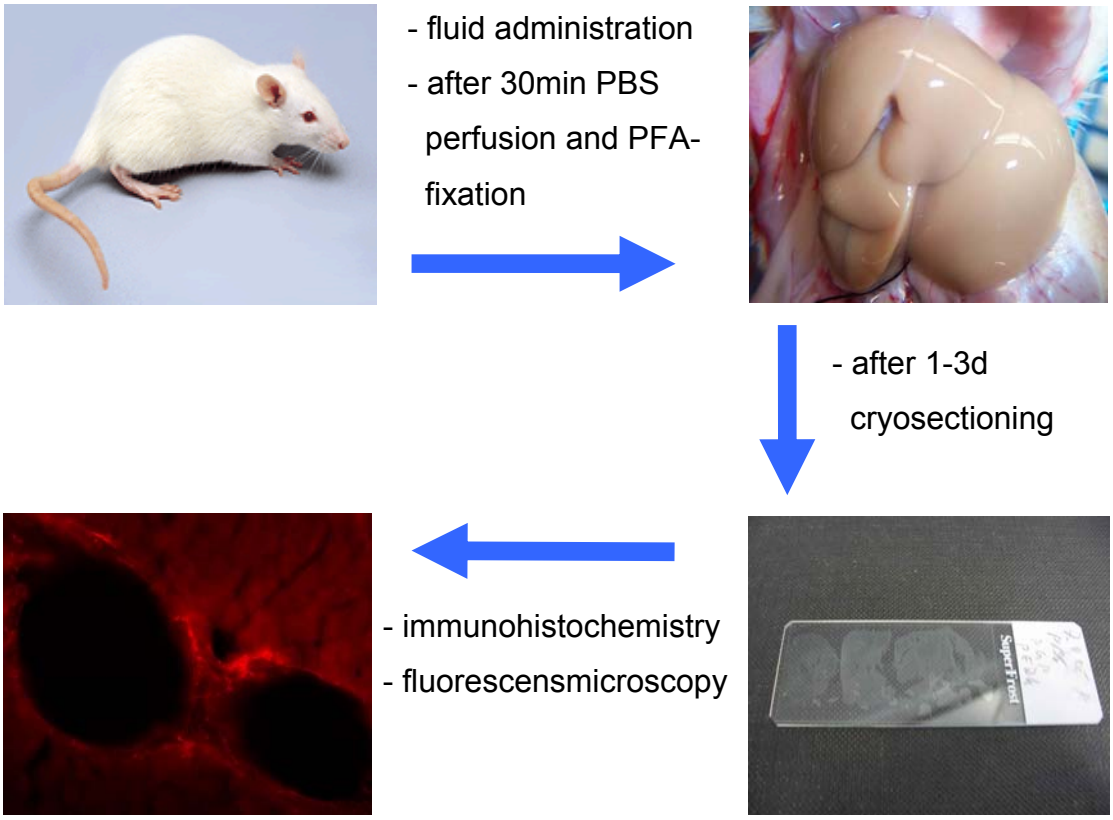

Figure 4: Experimental animal model to detect elevated ERK phosphorylation levels in neurons innervating the liver.

Preparing the sections

We established a rodent animal model to visualize osmosensitive neurons in the liver. For pERK immunostaining experiments mice were given 1ml fluid orally (water, PBS or water including 100µM ruthenium red) using an application cannula. 20min after fluid administration animals were anaesthetised by intraperitoneal injection of 0.2-0.5ml PBS containing 10mg/ml Ketavet (Pfizer) and 0.04% ROMPUN (Bayer), and were subsequently perfused with chilled (4°C) 4% paraformaldehyde (PFA) in

PBS. Immediately after perfusion, the tissue of interest was dissected and post-fixed in 4% PFA at 4°C for 30min (DRGs) up to 2 hours (Molliver, Wright et al.).

For dehydration, tissue was subsequently immersed in 25% sucrose in PBS for 1-3 days until the tissue sank to the bottom of the sucrose solution. The tissue was prepared for sectioning by placing it into TissueTek Cryomolds filled with OCT compound and freezing on dry ice. Sections were cut on a freezing microtome at 15µm (DRGs) or 20µm (Molliver, Wright et al.) (Molliver, Wright et al.) and collected on APES or gelatine coated slides. The tissue slides were stored at -20°C or immediatly processed for immunostaining.

Immunostaining of tissue sections

Tissue sections were pre-incubated in 1% serum albumin (BSA) and 0.3% Triton X-100 in TBS for 2h and incubated overnight at RT with primary antibodies (dillution 1:250 – 1:1000) in TBS with 0.3% Triton X-100 and 5% normal goat serum. For background control the primary antibody was left out. Tissue sections were washed by rinsing slides 3x for 10min in excess TBS and incubated for 2h at room temperature with secondary antibodies (double concentration of the primary antibody) in TBS containing 0.3% Triton X-100 and 5% normal goat serum. Tissue sections were washed 3x for 10min in excess TBS and then mounted in Aqua-Polymount. The slides were visualized using a Leica DM 5000B Upright Fluorescence Light Microscope and MetaVue Imaging Software.

2.2.5 Calcium Imaging

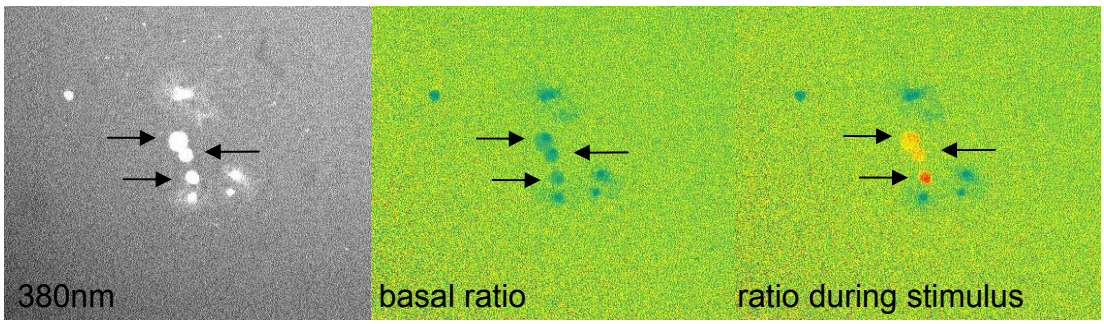

Figure 5: Calcium-imaging experiments
Images of DRG neurons during calcium-imaging experiments showing the Fura-2 fluorescence at 380nm and the 340/380 ratio image both before and during cell stimulation.

Cultured cells were loaded for 30min with 5µM of the membrane permeable fluorescent dye Fura-2. Cells were then transfered to the recording chamber containing extracellular buffer of isotonic osmolality (310mOsm/kg) of a fluorescence microscope (Zeiss Axiovert 200). Hypo-osmotic and drug (Ruthenium Red, Gadolinium) stimuli were applied using a gravity-driven multi barrel perfusion system (WAS02). Cells were illuminated alternately at 340nm and 380nm for 500ms and ratio images were collected every 1.6 seconds using MetaFluor Software (Visitron Systems) and a SPOT-SE18 CCD camera. All ratios were normalized to the mean of the first 10 ratio images (R_0) and plotted as R/R_0. At the end of each individual experiment cells were perfused with 40mM KCl for 16s. All cells that did not respond to the KCl stimulation were considered either non-neuronal cells or dead neurons and were therefore excluded from the analysis. The aquired data was analyzed using MetaFluor 7.01 software (Molecular Devices, Visitron Systems) and MS excel.

2.2.6 Whole-cell patch clamp

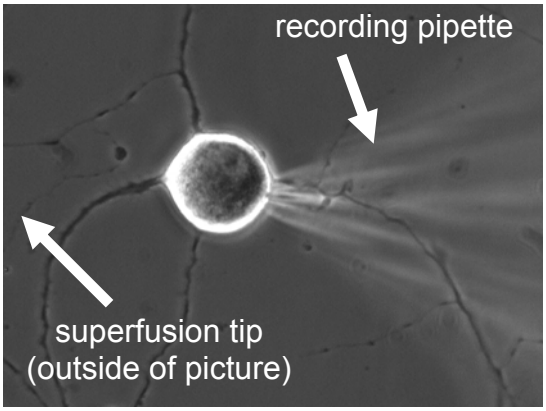

Figure 6: Whole-cell patch clamp experiments
Experimental setup for whole-cell electrophysiological studies.

Whole-cell recordings were made from DRG neurons 24-48 h after plating using patch pipettes with a resistance of 5-10 MΩ. Patch pipettes were pulled from borosilicate glass capillaries. The recording chamber contained extracellular buffer of isotonic osmolality (310mOsm/kg) and recording electrodes were filled with intracellular solution. Membrane current and voltage were amplified and acquired using an EPC-10 amplifier (HEKA) sampled at 10 kHz. For whole-cell recording, the membrane voltage was held at –60mV. Osmotic stimuli (250, 260, 270, 280 and 290mOsm/kg) were applied using a gravity driven multi-barrel perfusion system (WAS02). The outlet of the output capillary (400 µm inner diameter) was placed not more then 100µm away from the patched cells. Traces were acquired with PatchMaster and analyzed using FitMaster software (both HEKA).

2.2.7 Retrograde Labelling

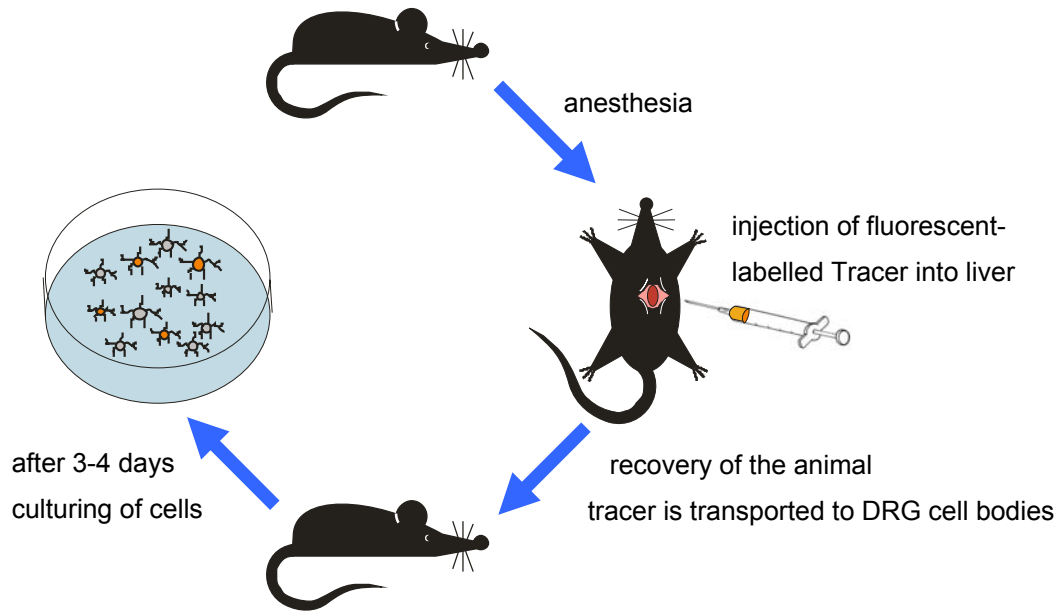

Figure 7: Retrograde labelling experiments.
Schema of marking liver-innervating neurons of the DRG via retrograde labeling.

For retrograde labeling experiments fluorophor-conjugated dextrans were used. Dextrans are hydrophilic polysaccharides synthesized by *Leuconostoc* bacteria. They are characterized by their high molecular weight, good water solubility, low toxicity and relative inertness. These properties make dextrans effective water-soluble carriers for dyes, indicators, and reactive groups in a wide variety of applications. Moreover, their biologically uncommon α-1,6-poly-glucose linkages are resistant to cleavage by most endogenous cellular glycosidases Therefore dextran conjugates make ideal long-term tracers for live cells. In this study anionic Alexa Fluor 488 conjugated Dextran 3000MW (Molecular Probe, Eugene) was used because of its small molecular weight which allows good peripheral neuronal processes penetration and fast diffusion.

Animals were anesthetized by intraperitoneal injection of 0.2-0.5ml phosphate-buffered saline (PBS) containing 10mg/ml Ketavet (Pfizer) and 0.04% ROMPUN (Bayer). To gain access to the liver a small incision of the abdominal skin and underlying muscle tissue was made. Several injections of 3 - 5µl to a total amount of 20µl of 2,5% Alexa-Fluor 488 coupled Dextranamin MW 3000 were made into the top liver lobes. The application needle was left inside the injection site for 30s before retraction to avoid dye leakage. Following the injection the wound was sutured, a local anesthetic (Xylocain-Gel) given and the animal put back into a cage and allowed to recover. Optimal labelling of the DRGs occurred 3 – 4 days post injection when the mice were sacrificed by CO_2 inhalation for cell culture.

2.2.8 Indirect calorimetry

Indirect calorimetric experiments were carried out at the Deutsches Institut für Ernährung in Potsdam-Rehbrücke (DIFE). Mice were kept in hermetically sealed cages. The volume of oxygen and carbon dioxide entering and exiting the cages was measured every six minutes to determine the volume of inhaled oxygen and expired carbon dioxide by the animals. One cage was left empty (no animals) and was used to determine control levels of entering out exiting gas. Mice were divided into three groups with 5 animals in each group. One group received an oral administration of 1ml of water, the next received an administration of 1ml of PBS and the last group received a sham administration. The administrations had to be done within a few minutes between acquisitions of two data points. Mice were kept in the cages during the whole experiment and data points were acquired from 9am in the morning until 17pm, the mice received their administration at 10am. The respiratory quotient and energy expenditure of the animals were calculated based on consumed oxygen and expired carbon dioxide levels.

3 Results

3.1 The physiological stimulus of water-drinking in mice

After water-drinking water passes through the small intestine, is absorbed into vessels of the splanchnic mesentery and collects in the hepatic portal vein. It then courses through the liver and exits through the hepatic vein into the vena cava becoming diluted in the general circulation. In order to see how large the peripheral physiological stimulus for hepatic osmosensitive afferents is, when a mouse drinks 1ml of water, it is necessary to take blood samples as close to the liver as possible following water intake. Animals received oral administration of 1ml of water at room temperature (RT) with an application cannula. After 30, 60 and 120 minutes mice were anesthetized and blood was taken from the portal vein with a syringe, followed by measuring the blood osmolality with a vapor pressure osmometer (Kreienbaum). The blood osmolality of animals that did not receive water administration was also analyzed to measure unstimulated blood osmolality levels (Figure 8). The basal blood osmolality in the mouse was found to be 310.0 +/- 2.1mOsm/kg (n=7). Thirty minutes after oral administration of 1ml of water blood osmolality within the portal vein decreased to 285.6 +/- 3.0mOsm/kg (n=5), which corresponds to an 8% decrease in blood osmolality. One hour after water-drinking, regulatory responses have already taken effect and the blood osmolality increased again to 291.5 +/- 2.6mOsm/kg (n=5). Two hours after water-drinking the blood osmolality had almost recovered to basal levels (304.1 +/- 1.9mOsm/kg; n=5).

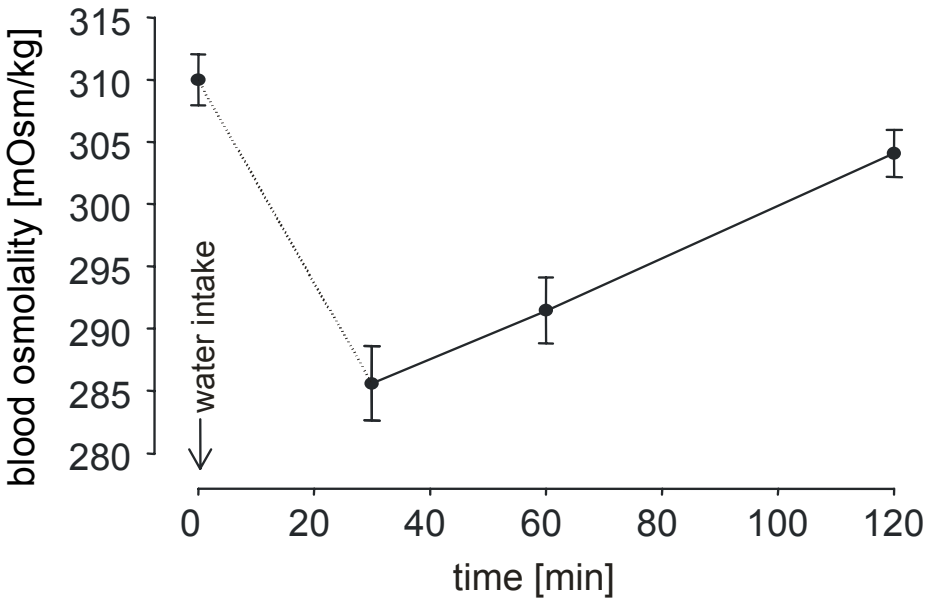

Figure 8: Diagram of blood osmolality change following water intake.
In order to determine the magnitude of the physiological stimulus of water-drinking in mice portal vein blood osmolality was measured before and at three time points (30, 60 and 120min) after the animals had received oral administration of 1ml of water.

3.2 An *in vivo* model to detect peripheral neuron activation

If there are peripheral afferents innervating the liver able to detect changes in osmolality then these neurons should be activated after water-drinking. They should have a sensitivity in the range described in Figure 8. In order to analyse osmotic stimulation of peripheral neurons we established an *in vivo* animal model based on the activation of the extracellular-signal regulated kinases 1 and 2 (ERK 1/2). ERK 1 and 2 have 83% amino acid identity and are expressed to various extents in all tissues (Roux and Blenis 2004). They belong to the mitogen-activated protein kinase (MAPK) protein family, which are widely conserved serine/threonine protein kinases involved in many cellular programs such as cell proliferation, differentiation, motility, and death

(Chen, Gibson et al. 2001). ERK 1/2 have two phosphorylation sites (p44/42) and become rapidly activated upon phosphorylation by a variety of extracellular signals such as mitogens, growth factors, cytokines and also osmotic stress (Lewis, Shapiro et al. 1998).

To detect hypotonicity evoked activation of liver innervating afferents, mice received an administration of 1ml of water applied with an application cannula. Twenty minutes after administration animals were perfused with PBS and fixed with 4% paraformaldehyde (PFA), the liver was removed and tissue sections prepared. An antibody against the phosphorylated (activated) form of ERK 1/2 (pERK) was then used as a rapid marker of peripheral nerve activation in the liver and was visualized by immunostaining. Figure 9 shows fluorescence micrographs of pERK stained liver sections. pERK stained nerve fibers were observed to mainly innervate the surroundings of liver blood vessels as can be seen in the top left image. Their neuronal nature was confirmed by co-immunostaining with the neuronal marker PGP9.5 (bottom left and merged right).

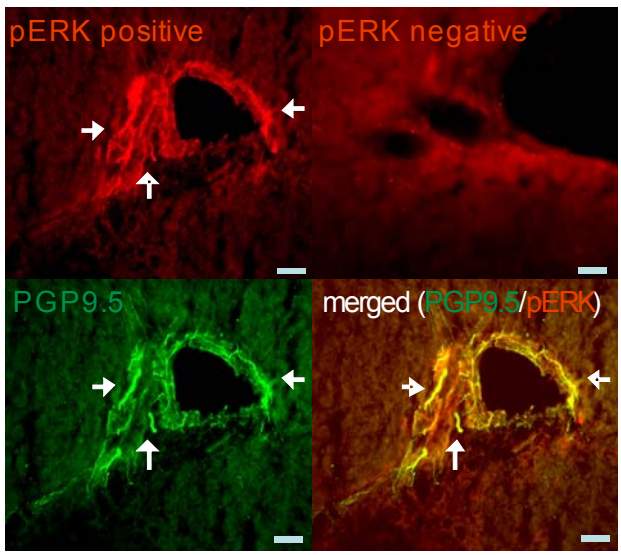

Figure 9: Hepatic neurons become activated following water intake.
Fluorescence micrographs of liver blood vessels. Upper two images show blood vessels with innervation of pERK stained neurons (left) and without (right). Bottom two images show the same blood vessel as top left stained with the neuronal marker PGP9.5 (left) and merged (right). Arrows indicate stained neuronal fibers. Scale bar: 50µm.

ERK activation occurs not only in response to osmotic stimuli, but also various other stimuli. In order to quantify ERK activation following hypo-osmotic stimuli (administration of 1ml of water), two controls were needed: a sham administration to exclude stress effects due to the procedure itself and administration of the same volume of phosphate buffered saline (PBS) to exclude volume effects. PBS had an osmolality of 304.5 +/- 3.0mOsm and was slightly hypoosmotic compared to mouse blood osmolality. After immunostaining, the number of blood vessels that showed innervation by neuronal fibers positively stained for pERK was counted. As shown in Figure 10A the number of blood vessels innervated by pERK stained neurons increased significantly following water-drinking compared to both control groups. Under sham conditions 23.4% +/- 6.0% of the liver blood vessels show pERK staining (n=7, 22/107 analyzed blood vessels). The number of pERK stained vessels increased to 34.6% +/- 7.9% (n=6, 31/100 blood vessels) following PBS administration, but this increase is not significantly different compared to sham treatment. However after water-drinking 51.7% +/- 7.4% show pERK staining (n=7, 64/125 blood vessels), which is a significant increase compared to both sham and PBS groups ($p<0.01$ compared to sham, $p<0.05$ compared to PBS; t-test). The only difference between the PBS- and water-drinking groups is the osmolality of the solution administered and therefore the increase of pERK staining by ~17% is likely to be the consequence of hypotonic stimulation.

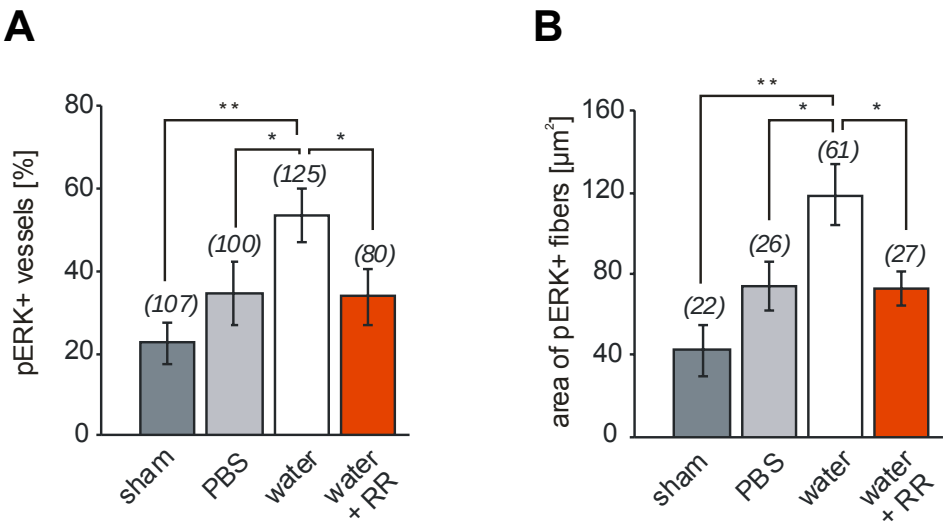

Figure 10: Quantification of ERK activation in the liver
A, quantification of liver blood vessels being innervated by pERK stained fibers after sham administration and administration of 1ml of PBS, water and water including 100µM Ruthenium Red (RR). Numbers above bars indicate analyzed blood vessels. **B**, graph shows the calculated area of pERK stained fibers innervating liver blood vessels, same treatment groups as A. Numbers above bars indicate analyzed blood vessels.

The basal level of pERK stained neurons (~23% under sham conditions) demonstrates that there is always some ERK activation in neurons innervating hepatic blood vessels. However, following hypotonic stimulation it would appear that these neurons become more activated as shown by increased pERK staining, or additional recruitment of neurons, which become pERK positive after such treatment. In Figure 10A every hepatic blood vessel positively stained for pERK was counted independently of the amount of stained fibers surrounding the respective vessel. Focusing only on pERK stained hepatic blood vessels the amount of pERK staining was quantified by calculating the area of pERK stained fibers innervating those blood vessels. Figure 10B demonstrates a significant increase of the area of pERK stained neuronal fibers following water-drinking (118.6µm^2 +/- 14.9µm^2) compared to both sham (42.2µm^2 +/- 13.0 µm^2; $p<0.01$; t-test) and PBS administration

(73.58μm^2 +/- 11.8μm^2; $p<0.05$; t-test). Here the PBS group shows also a significant increase of the area of pERK stained neuronal fibers compared to sham ($p<0.05$; t-test). Comparing the PBS and water-drinking groups, 60% of the increase in the stained area is an osmotic effect.

Members of the TRP-channel family are reported to be osmosensitive and maybe involved in osmosensation suggesting that they are candidates for peripheral osmosensors (Strotmann, Harteneck et al. 2000; Suzuki, Mizuno et al. 2003; Reiter, Kraft et al. 2006). If that is the case, then the observed increase of ERK activation after water-drinking should not take place if the water administered contains 100μM ruthenium red (RR), a non-selective TRP-channel inhibitor (Clapham, Julius et al. 2005). Indeed, the number of hepatic blood vessels being innervated by pERK stained neurons is significantly lower in animals that received water containing RR (Figure 10A; 33.7% +/- 6.6%; n=7; $p<0.05$; t-test). The area of pERK stained neuronal fibers following water-drinking containing RR is also significantly lower than in the water-administration group (Figure 10B; 72.7μm^2 +/- 8.3μm^2; $p<0.05$; t-test). These results suggest the involvement of a TRP channel in peripheral osmosensation, which will be further studied (see 3.4).

3.3 Calorimetric experiments

Employing calorimetric experiments it was reported that water-drinking leads to an increase in energy expenditure in human subjects (Boschmann, Steiniger et al. 2003). To test whether this observation can be verified in mice indirect calorimetric experiments were carried out at the Deutsches Institut für Ernährung (DIFE) in Potsdam-Rehbrücke. Animals were kept in hermetically sealed cages in which the incoming and outgoing oxygen and carbon dioxide

levels were measured for the duration of the experiment. Mice received 1ml of water orally and control groups received 1ml PBS or sham administration. Both respiratory quotient and energy expenditure were calculated based on consumed oxygen and expired carbon dioxide levels of the animals. Figure 11A shows the respiratory quotient, a measure indicating the type of metabolite which is mainly metabolized (a value of 1 meaning pure carbohydrate oxidation; a value of 0.7 meaning pure fat oxidation). Figure 11B shows the energy expenditure of the animals. The energy expenditure values were normalized against each animals baseline values measured before starting the experiment due to variation across animals. Both the respiratory quotient and energy expenditure increased in all three groups following the respective administrations. There was no significant difference between the three groups regarding either the increase in the respiratory quotient or the increase in energy expenditure (n=15, t-test). The stress due to the procedure itself (taking the animal out of the cage, handling of the animal and oral administration) leads to a robust increase in the respiratory quotient and energy expenditure which may obscure any effect that water-drinking may have (see sham in Figure 11).

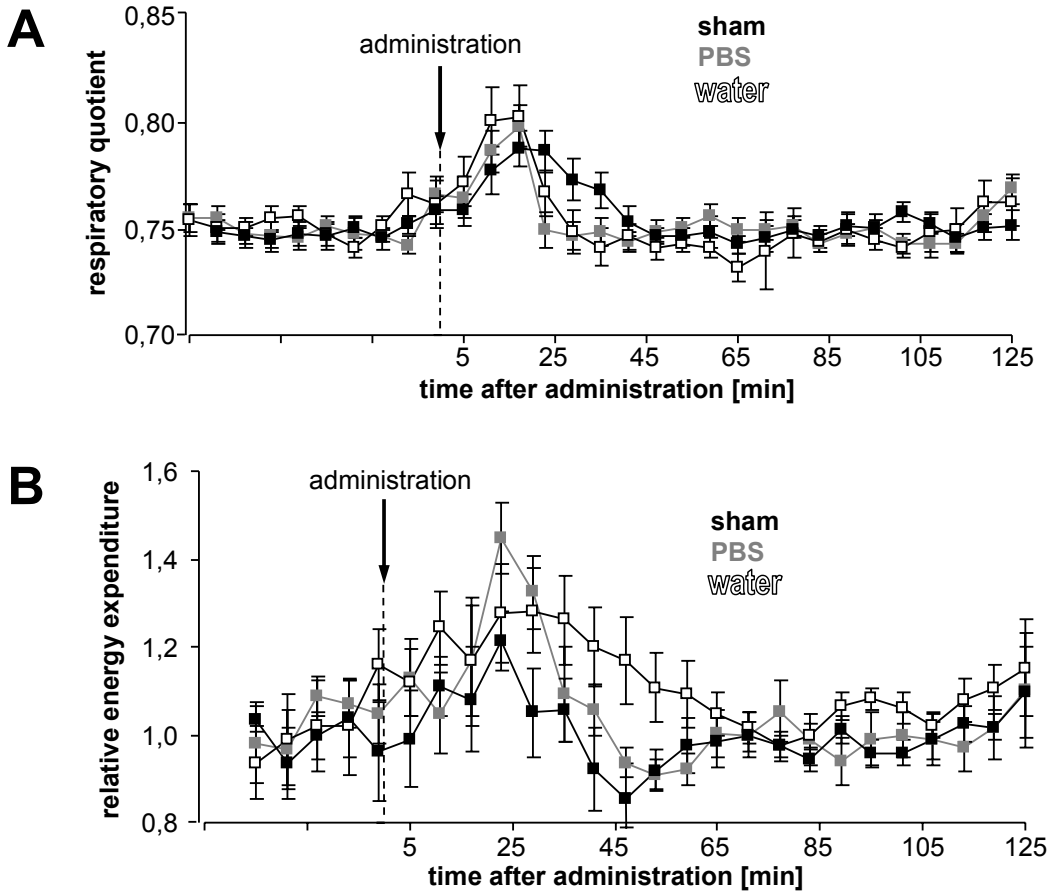

Figure 11: calorimetric measurements following water intake
A, diagram of the respiratory quotient for all three groups (sham, PBS and water). Arrow marks when animals received sham, PBS or water administration. **B**, diagram showing normalized energy expenditure levels. Arrow marks when animals received sham, PBS or water administration.

3.4 Osmosensitivity of sensory neurons in the dorsal root ganglia

3.4.1 DRG neurons in the thoracic region are highly osmosensitive

Somatic and visceral sensory neurons have their cell bodies in the dorsal root ganglia (DRG) and axonal processes in the periphery and spinal cord. It has been reported that the liver is innervated by afferents from DRGs located

in the thoracic region of the spinal cord, specifically the region of T7-T13 (Magni and Carobi 1983; Berthoud 2004). We therefore hypothesized that DRGs from the thoracic region are more osmosensitive compared to DRGs in cervical or the lumber region. Parasympathetic innervation of the upper abdominal organs, including the liver, is provided by the vagus nerve whose afferent neurons are located in the nodose ganglia (Magni and Carobi 1983; Berthoud, Kressel et al. 1992). Cells from parasympathetic nodose ganglia of the vagus nerve were therefore also analyzed to see whether osmosensation may be mediated through the sensory or vagal neurons. DRGs from different spinal regions (cervical C4-C7, thoracic T7-T13, and lumbar L1-L6) and nodose ganglia of adult 8 – 12 week old mice were dissected and cultured. 24 hours later cultured neurons were loaded with the Ca^{2+}-sensitive dye Fura-2 and the osmosensitivity was studied employing Ca^{2+}-imaging. Figure 12A shows a typical cellular Ca^{2+}-response following a hypotonic stimulus of 230mOsm which was applied using a gravity driven multi-barrel perfusion system. The osmolality of the bath solution was at the same level of 310mOsm as measured within the portal vein of mice (see chapter 3.1 and Figure 8). At the end of each Ca^{2+}-imaging experiment 40mM KCl was applied. A high extracellular concentration of K^+ ions depolarizes neurons and leads to a Ca^{2+} response due to Ca^{2+}-influx through voltage gated Ca^{2+}-channels. All cells that did not respond to the KCl stimulation were considered either non-neuronal cells or dead neurons and were therefore excluded from the analysis. The proportion of cells from each region that responded following osmotic stimulation was then quantified (Figure 12B). Among cells from the thoracic region a significantly larger population of cells was found to be osmosensitive (30.9%: n=8, 51/165 cells) compared to cervical DRGs (11.3%; n=7, 18/160 cells; $p<0.001$), lumbar DRGs (9.1%; n=7, 19/208 cells; $p<0.001$) or to cells from nodose ganglia (9.9%; 8/81 cells; $p<0.001$, all tested with chi-square test). When stimulating thoracic neurons three times successively for 15s there was no significant difference in the magnitude of the response, so the osmotically evoked responses did not exibit stimulation dependent sensitization or desensitization (Figure 12C + D, n=10).

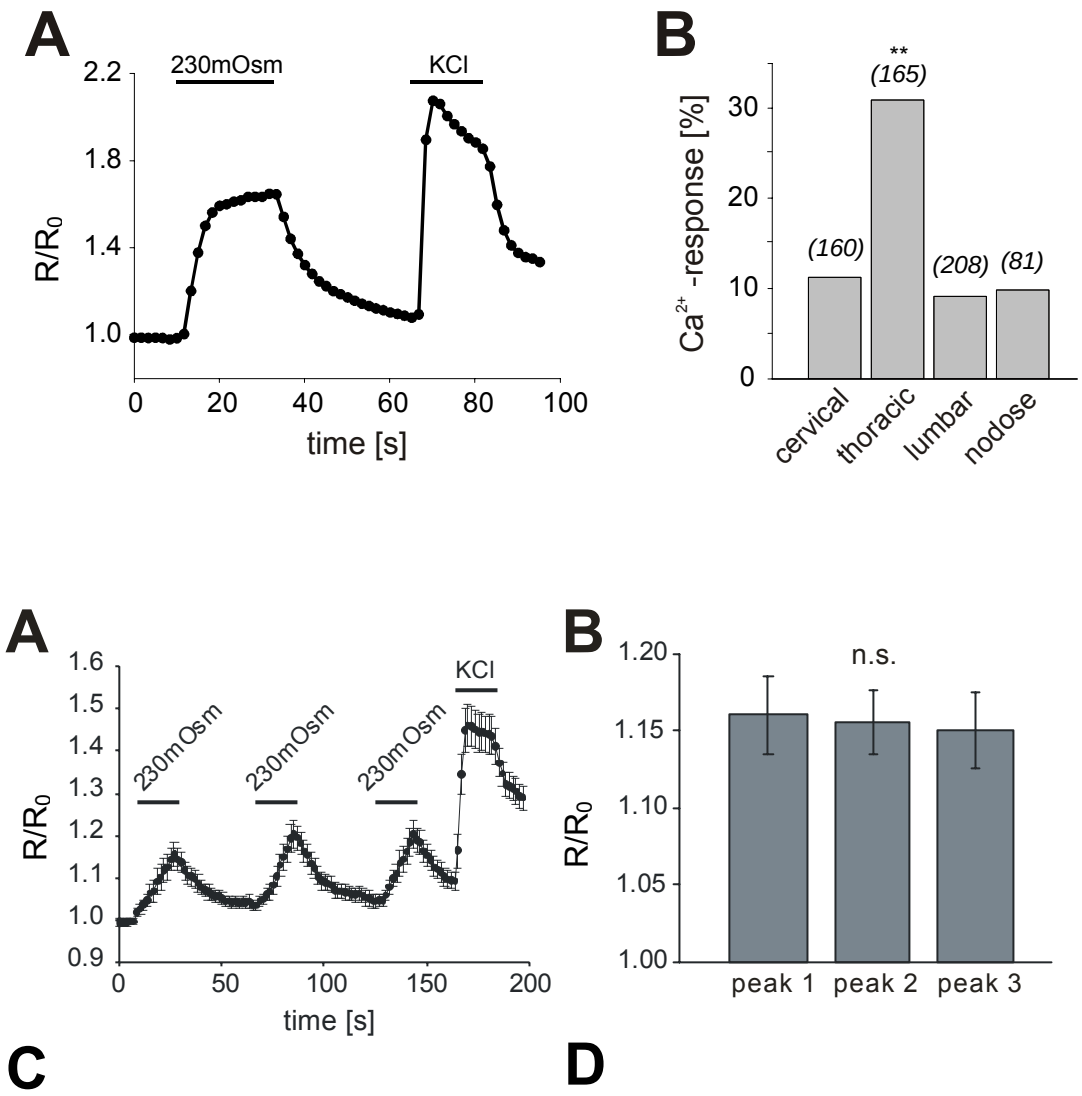

Figure 12: Thoracic DRG neurons are highly osmosensitive
A, trace showing the response of a thoracic DRG neuron to a 230mOsm stimulus of 22s duration in Ca^{2+}-imaging experiments, KCl is used as positive control. Osmolality of the bath: 310mOsm. **B**, quantification of the Ca^{2+}-responses of DRG neurons from the cervical, thoracic and lumbar region as well as of cells from the nodose ganglion. Numbers above bars indicate analyzed cells. **C**, averaged Ca^{2+}-responses of thoracic DRG neurons challenged 3 times successively with a 230mOsm stimulus, KCl is used as positive control. **D**, quantification of the 3 stimuli.

3.4.2 Cell swelling due to hypotonicity

When neurons are exposed to hypotonicity water flows across the cell membrane leading to an increase in cell volume. The effects of water influx and the associated change in volume might modulate the activity of osmosensitive channels. Specifically, the dilution of a cytoplasmatic solute, a change in intracellular ionic strength or membrane stretch might modulate osmoreceptors (Bourque 2008). Most studies support the mechanical gating (stretching of the cells membrane) due to cell swelling as the activating mechanism of osmoreceptors (Oliet and Bourque 1993; Viana, de la Pena et al. 2001; Zhang, Kindrat et al. 2007).

When thoracic DRG neurons were challenged with a hypotonic stimulus of 230mOsm, a change in cell diameter of 7.3% was observed, which corresponds to an increase of the area by 15.8% (Figure 13, n=2, 6 cells analyzed). Cells increased in size reaching their maximum 8-9 seconds following stimulation and after removal of the stimulus their cell diameter decreased back to their normal size after 10-12 seconds.

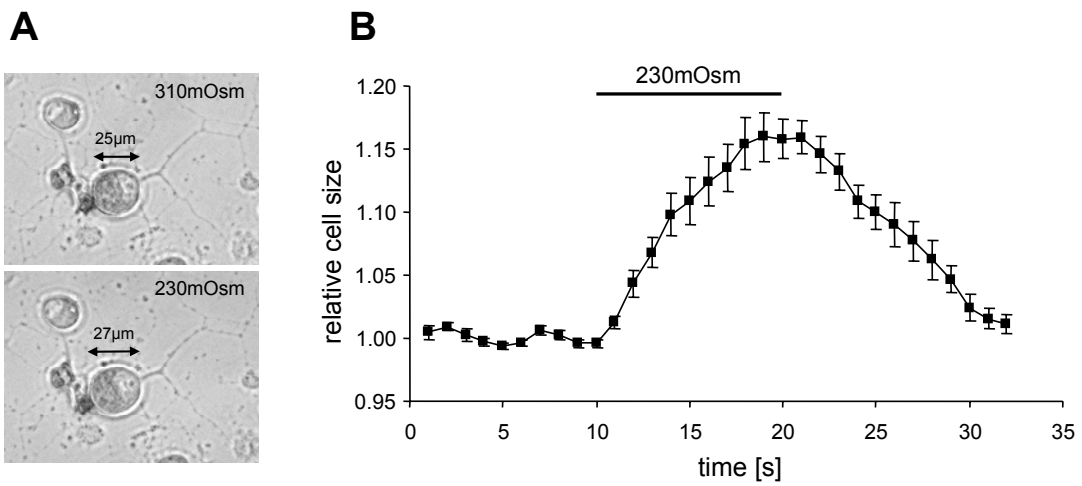

Figure 13: Hypotonicity induced cell-swelling
A, bright field images showing the same cell resting at 310mOsm and during hypotonic challenge of 230mOsm, arrow bar indicates cell diameter. **B**, diagram showing the relative increase of the calculated cell area during a 20s 230mOsm stimulus.

3.4.3 Osmosensitive neurons are IB4 negative

DRG neurons can be roughly divided into two main subpopulations: small and large neurons. The large neurons are thought to be mainly involved in mechanoreception while most small neurons are involved in nociception (Lewin and Moshourab 2004). Small DRG neurons can be further subclassified into nerve growth factor (NGF)-dependent neurons expressing the NGF receptor tyrosine kinase A (TrkA) and the glial cell line-derived neurotrophic factor (GDNF)-dependent neurons expressing the GDNF receptor (Silverman and Kruger 1990; Snider and McMahon 1998; Stucky and Lewin 1999). NGF-responsive neurons contain neuropeptides such as Substance P and calcitonin gene-related peptide (CGRP) (Averill, McMahon et al. 1995) whereas GDNF-dependent neurons lack neuropeptides but bind isolectin B4 (IB4) derived from *Griffonia simplicifolia* (Molliver, Wright et al. 1997; Bennett, Michael et al. 1998). Thus, the types of DRG neurons can also be distinguished by immunoreactivity.

Figure 14A shows fluorescence micrographs of hepatic blood vessels from mice that received 1ml water before they were fixed and perfused. For subclassification of osmosensitive hepatic afferents, liver sections were stained for pERK and IB4, but no co-immonustaining was observed. Next the functionality of IB4-positive neurons was studied. Fura-2 loaded thoracic DRG neurons were stained with IB4 prior to Ca^{2+}-imaging experiments and their Ca^{2+}-responses to a 230mOsm stimulus was quantified (Figure 14B). Looking at all cells an expected proportion of 28.8% (n=7, 32/111 cells) was found to be osmosensitive (compare to Figure 12B). But when focusing on IB4 stained neurons a significantly smaller number of cells responded to the hypotonic stimulus (7.7%, n=7, 7/91 cells; $p<0.01$, chi-square test).

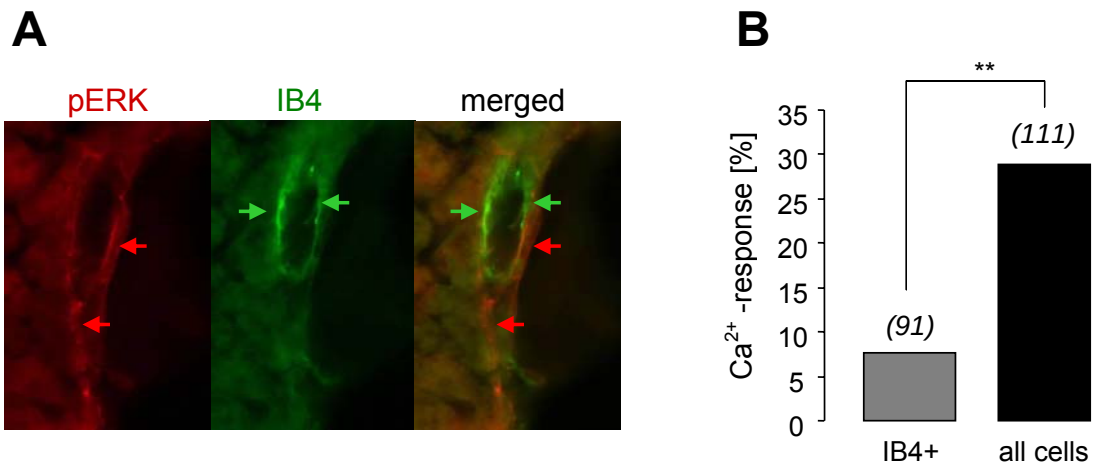

Figure 14: The osmosensitive neurons are IB4-negative
A, fluorescence micrographs of liver blood vessels from an animal that drank 1ml of water, stained for pERK and IB4 (left two images). The overlay is shown in the right image. Arrows indicate fibers stained for pERK (red) and IB4 (green) respectively. **B**, quantification of the Ca^{2+}-responses of thoracic DRG neurons. Left column shows only cells positively stained for IB4, right column shows all cells. Numbers above bars indicate analyzed cells.

3.4.4 Hypotonicity evokes an inward current in thoracic DRG neurons

In order to study how thoracic DRG neurons respond to different magnitudes of hypotonic stimuli we conducted whole-cell patch clamp recordings. Experiments were performed on cultured thoracic DRG neurons (T7-T13) twenty four hours after plating. The bath solution was 310mOsm and osmotic stimuli from 260 to 290 mOsm were applied using a gravity driven multi-barrel perfusion system. A high proportion of neurons was found to exibit inward currents under voltage clamp conditions when osmotically challenged (67.6%; n=7, 25/37 cells). As shown in Figure 15A this osmotically evoked inward current increases in amplitude with increasing hypotonicity of the stimuli. The osmolality at which the half maximum effect of the hypotonic

stimulus was reached was calculated to be 278mOsm (Figure 15B). Amplitudes were normalized against each cells mean amplitude at two separate 260mOsm stimuli, which were given before and after each 270, 280 and 290mOsm stimulation. Note that 278mOsm is a value well within the physiological range (see also Figure 8).

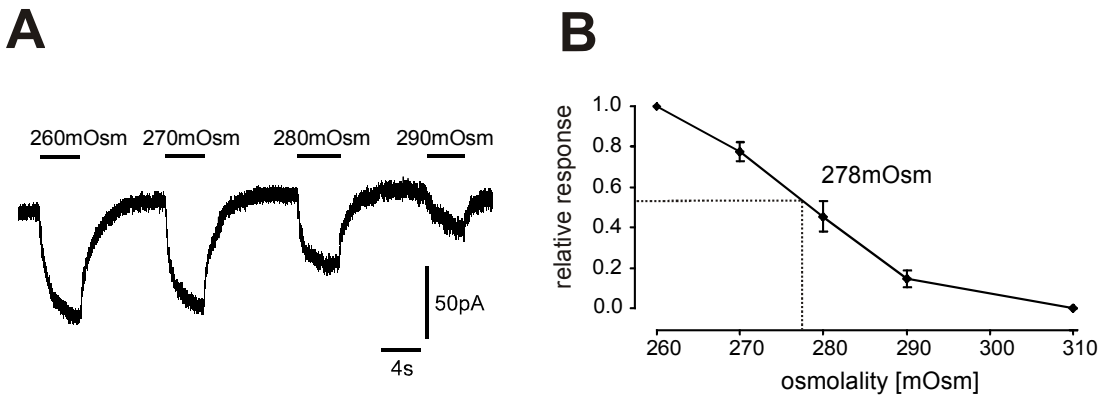

Figure 15: Hypotonicity evokes an inward current
A, whole-cell recording trace of a thoracic DRG neuron that is challenged successively with hypotonic stimuli (260, 270, 280, 290mOsm; bath osmolality: 310mOsm). **B**, diagram indicating the osmolality where the half maximum effect (amplitude) is reached. Responses are normalized against each cells mean amplitude of two 260mOsm stimli (one before and after each stimulation with 270, 280 and 290mOsm).

3.5 Summary

The physiological stimulus of water-drinking was analyzed. When a mouse drinks 1ml of water the blood osmolality in the hepatic portal vein area decreases by 8% from 310mOsm to 285mOsm within thirty minutes. This hypo-osmotic stimulus is sufficient to lead to a significant increase in the phosphorylation of ERK in liver innervating neurons. Drinking the same volume of PBS solution did not have the same effect. Indirect calorimetric experiments did not show an effect of water-drinking upon respiratory quotient or energy expenditure, presumably due to a high response of the animals to the procedure itself.

Employing calcium imaging experiments a significantly larger proportion of cells from thoracic DRG neurons were found to be osmosensitive compared to cervical and lumbar spinal regions which do not innervate the liver. This was also found compared to parasympathetic neurons from nodose ganglia of the vagus nerve. A 230mOsm hypotonic stimulus provokes an increase in cell size reaching a maximum after 8-9 seconds. The osmosensitive cells appear to belong to an IB4-negative population as the proportion of osmosensitive cells is absent in IB4-positive neurons. Whole-cell patch clamp recordings demonstrated that a hypotonic stimulus evokes an inward current in osmosensitive cells. The inward current increases in amplitude depending on the magnitude of hypotonicity of the stimulus evoking a half maximum osmotic effect in a range of physiological relevance (278mOsm).

3.6 TRPV4's role in osmosensation

3.6.1 TRPV4 -/- mice phenotype

TRPV4 -/- mice were obtained from Makoto Suzuki and Masashi Imai, Department of Pharmacology, Jichi Medical School, Japan. The animals received an oral administration of 1ml of water with an application cannula. After 30, 60 and 120 minutes blood was taken from the portal vein and the blood osmolality was immediately measured using a vapor pressure osmometer (Kreienbaum). To determine basal osmolality levels, blood was taken from animals that did not receive water administration.

Measures of the blood osmolality in the portal vein of mice lacking TRPV4 revealed that these animals are hyper-osmolar (316.4 +/- 1.8mOsm/kg; n=5) compared to TRPV4 +/+ animals (Figure 16; $p<0.05$, t-test) as has been reported by others (Liedtke and Friedman 2003). Thirty minutes after oral administration of 1ml of water the portal vein blood osmolality decreased to 298.7 +/- 1.3mOsm/kg (n=5) corresponding to a drop in blood osmolality of ~6%. For comparison, TRPV4 +/+ mice reached 285.6 +/- 3.0mOsm/kg thirty minutes after water administration, which means that TRPV4 -/- mice receiving the same osmotic stimulus as TRPV4 +/+ mice do not reach the same level of portal vein blood osmolality as TRPV4 +/+ mice ($p<0.01$, t-test). One hour after water-drinking, TRPV4 -/- blood osmolality went up again to 302.9 +/- 1.0mOsm/kg (n=5) and two hours after water-drinking it recovered back to basal levels (313.4 +/-2.0mOsm/kg; n=5). Thus TRPV4 -/- animals having received an hypotonic stimulus appear to be able to regulate their blood osmolality back to resting levels within the same time span as TRPV4 +/+ mice, but their blood osmolality is always shifted towards hyperosmotically compared to TRPV4 +/+ mice.

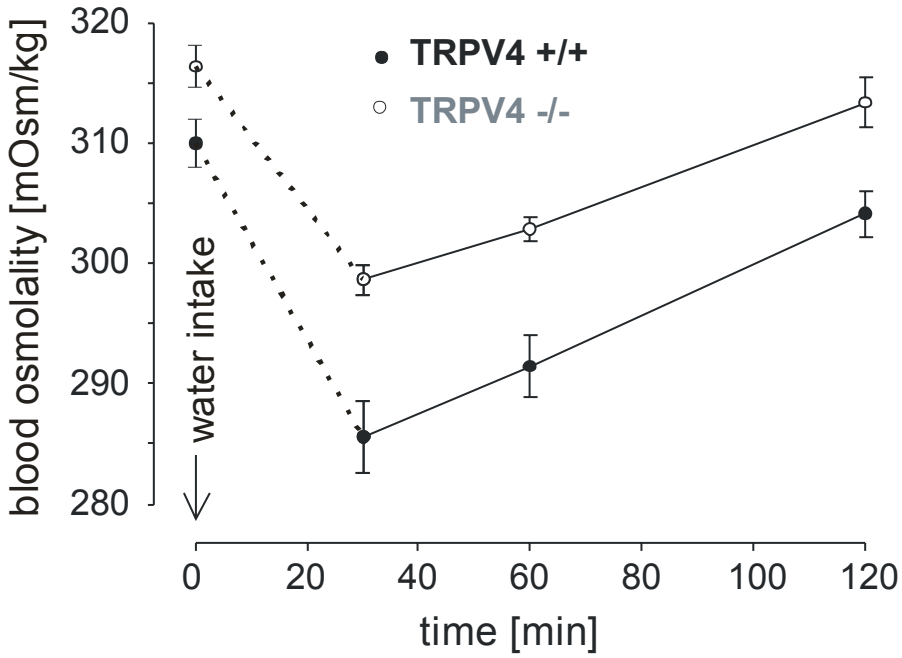

Figure 16: TRPV4 -/- mice are hyperosmolar compared to TRPV4 +/+ mice
Osmolality of portal vein blood was measured before and at three time points (30, 60 and 120min) after the animals received an oral administration of 1ml of water.

3.6.2 pERK levels do not increase in TRPV4 -/- animals

As described in chapter 3.2 and Figure 9, ERK gets phosphorylated in hepatic afferents following oral water administration. If TRPV4 plays a crucial role in hepatic osmosensation then water-drinking should not lead to an increase in ERK activation of liver innervating neurons in TRPV4 -/- mice. To detect activation of hepatic afferents TRPV4 -/- mice received an administration of 1ml of water. Twenty minutes after water-drinking animals were perfused and fixed, the liver removed and tissue sections prepared. Peripheral nerve activation of hepatic afferents was visualized by immunostaining with an antibody against the phosphorylated form of ERK (pERK). Figure 17A shows that the pERK level of TRPV4 -/- mice does not increase following a hypotonic stimulus and there was no significant

difference in the number of hepatic blood vessels innervated by pERK stained neurons between all three groups (sham group: 51.7% +/- 4.6%; n=6, 53/104 analyzed blood vessels; PBS group: 47.1% +/- 1.7%; n=6, 47/99 vessels; water group: 51.0% +/- 2.8%; n=6, 51/100 vessels). Focusing only on pERK stained hepatic blood vessels, the amount of pERK staining was quantified by calculating the area of pERK stained fibers innervating an hepatic blood vessel. As Figure 17B shows there was no significant difference in the area of pERK stained fibers between all three groups (sham group: 44.4µm^2 +/- 3.9µm^2; PBS group: 40.4µm^2 +/- 3.6µm^2; water group: 45.6µm^2 +/- 6.3µm^2; t-test). These results point toward a role of TRPV4 in osmosensation. However, one has to consider that due to the fact that TRPV4 -/- animals are slightly hyperosmolar and the *in vivo* physiological osmotic stimulus following water-drinking does not reach the same low threshold as in TRPV4 +/+ animals (see Figure 16). If the osmoreceptor needs a certain osmolality threshold for activation, this threshold might not be reached in TRPV4 -/- mice.

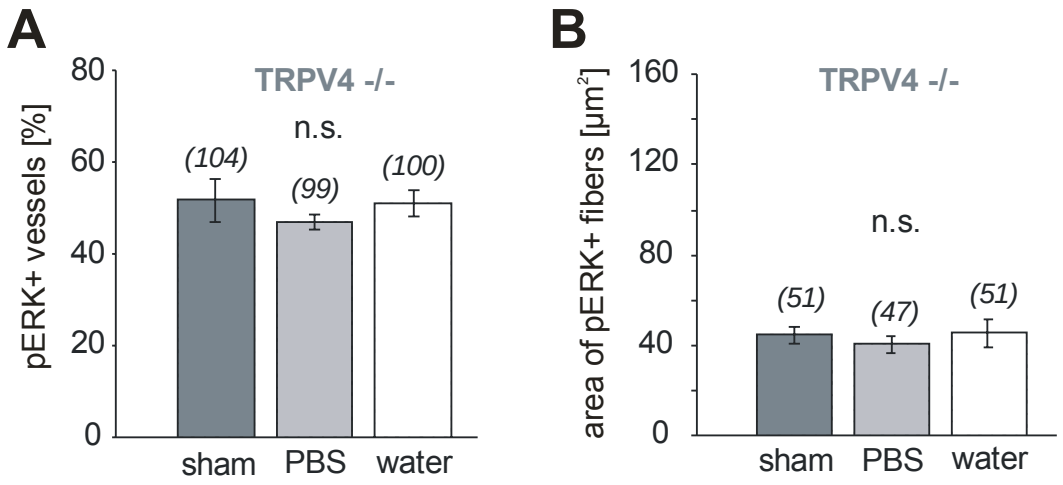

Figure 17: Quantification of ERK activation in TRPV4 -/- animals
A, quantification of hepatic blood vessels from TRPV4 -/- mice innervated by pERK stained fibers showing no significant difference in all three groups (sham administration, administration of 1ml of PBS or water). Numbers above bars indicate analyzed blood vessels. **B**, graph shows the calculated area of pERK stained fibers innervating hepatic blood vessels from TRPV4 -/- mice, same treatment groups as B. Numbers above bar indicate analyzed blood vessels.

3.6.3 Loss of osmosensitivity in thoracic TRPV4 -/- DRG neurons

If TRPV4 is involved in peripheral osmosensation then there should be a lack of osmosensing DRG neurons especially in the thoracic region of TRPV4 -/- mice compared to TRPV4 +/+ animals. DRGs from the cervical (C4-C7), thoracic (T7-T13) and lumbar (L1-L6) spinal regions of adult 8 – 12 week old mice were dissected and cultured. Twenty four hours after plating cultured neurons were loaded with Fura-2 and osmosensitivity was analyzed using Ca^{2+}-imaging experiments. The proportion of cells from each region that responded to hypo-osmotic stimulation was quantified (Figure 18). TRPV4 +/+ cells of the thoracic region contain significantly more osmosensitive cells (30.9%, n=8, 51/165 cells) compared to thoracic cells from TRPV4 -/- mice (10.8%; n=6, 30/279 cells; $p<0.001$, chi-square test). This loss of osmosensitivity was only observed in cells of the thoracic region. No significant difference was found in the number of cells responding to a hypotonic stimulus in the cervical (TRPV4 +/+: 11.3%; n=7, 18/160 cells; TRPV4 -/-: 6.9%; n=6, 14/202 cells) or lumbar region (TRPV4 +/+: 9.1%; n=7, 19/208 cells; TRPV4 -/-: 8.7%; n=6, 16/184 cells). It is interesting to note that there was also no significant difference in the number of cells responding to a hypotonic stimulus (around 10%) in cultures from thoracic TRPV4 -/- DRGs and those in cervical DRGs (both TRPV +/+ and -/-) and lumbar DRGs (both TRPV +/+ and -/-) suggesting a non-TRPV4 osmosensor may be responsible for this 10% response.

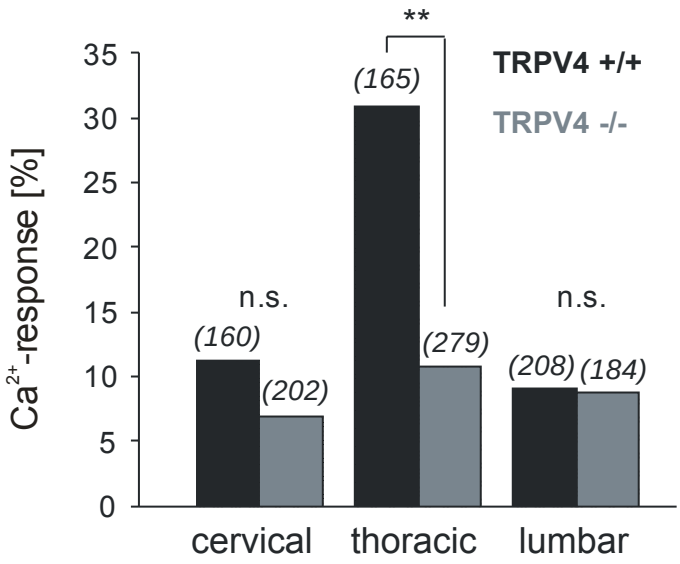

Figure 18: Lack of osmosensitive cells in thoracic TRPV4 -/- DRGs
Quantification of the Ca^{2+}-responses of DRG neurons from the cervical, thoracic and lumbar region from TRPV4 +/+ and TRPV4 -/- mice. Cells were challenged with 230mOsm for 22s (bath osmolality: 310mOsm). Numbers above bars indicate analyzed cells.

3.6.4 TRP-channel blockers inhibit osmotically evoked responses in Ca^{2+}-imaging experiments

The response of thoracic DRG neurons of TRPV4 +/+ mice to a hypotonic stimulus can by significantly inhibited by blockers such as ruthenium red (RR) or gadolinium (Gd^{3+}) (Clapham, Julius et al. 2005). The setup for Ca^{2+}-imaging experiments was similar to that described in chapter 3.4.1. Cells were first challenged with 230mOsm and then superfused with the inhibitor to ensure optimal inhibition during the second application of the 230mOsm stimulus, this time in the presence of the inhibitor (Figure 19A and C). An average from 5 data points prior to each hypotonic stimulus was set as $R/R_0=1$ due to variations in baseline levels for the first and second stimulus applications. As Figure 19B demonstrates the peak response during hypotonic stimulation ($R/R_0=1.15$ +/- 0.01; n=18) is significantly inhibited

when RR is present during the stimulation (R/R_0=1.01 +/- 0.01; p<0.01, t-test). Gd^{3+} had the same effect (Figure 19D), the peak response (R/R_0=1.25 +/- 0.05; n=18) was also significantly inhibited (R/R_0=1.01 +/- 0.04; p<0.01, t-test). These findings support the role of TRP or stretch activated channels being involved in peripheral osmosensation.

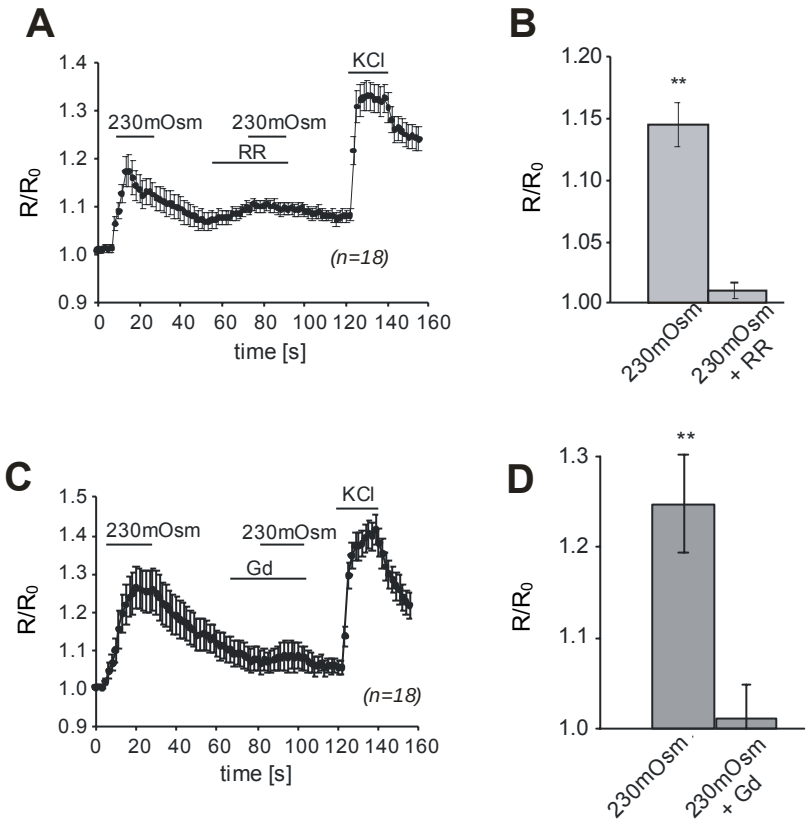

Figure 19: TRP-channel inhibitors block hypo-osmotically evoked response
A, averaged Ca^{2+}-responses of TRPV4 +/+ thoracic DRG neurons challenged with a 230mOsm stimulus and showing inhibition by 100µM Ruthenium Red (RR); n=18. KCl is used as positive control. **B**, quantification of the inhibition by RR. **C**, averaged Ca^{2+}-responses of thoracic DRG neurons challenged with a 230mOsm stimulus and showing inhibition by 100µM Gadolinium (Gd^{3+}); n=18. KCl is used as positive control. **D**, quantification of the inhibition by Gd^{3+}.

3.6.5 TRPV4 is expressed in all spinal regions as well as in the nodose ganglia

In Ca^{2+}-imaging experiments we found a higher proportion of DRG neurons in the thoracic spinal region to be osmosensitive compared to cervical or lumbar neurons and also compared to cells of the nodose ganglia. Furthermore this osmosensitive population was absent in TRPV4 -/- mice (chapter 3.6.3 and Figure 18). We therefore hypothesized that TRPV4 might be expressed at higher levels in thoracic DRGs. To test this DRGs from cervical, thoracic and lumbar spinal regions as well as nodose ganglia were collected and RNA was isolated (RNeasy mini kit, Qiagen). After the reverse transcription reaction (SuperScript II Reverse Transcriptase, Invitrogen) the synthesized cDNA was used as template for Real-Time PCR experiments to determine TRPV4 expression levels. Individual RNA expression levels have been normalized against two housekeeping genes (hypoxanthine phosphoribosyltransferase (HPRT) and Cyclophilin D). TRPV4 is expressed in all analyzed DRG regions as well as in the nodose ganglia and there was no significant difference in the expression levels (Figure 20; n=3; t-test).

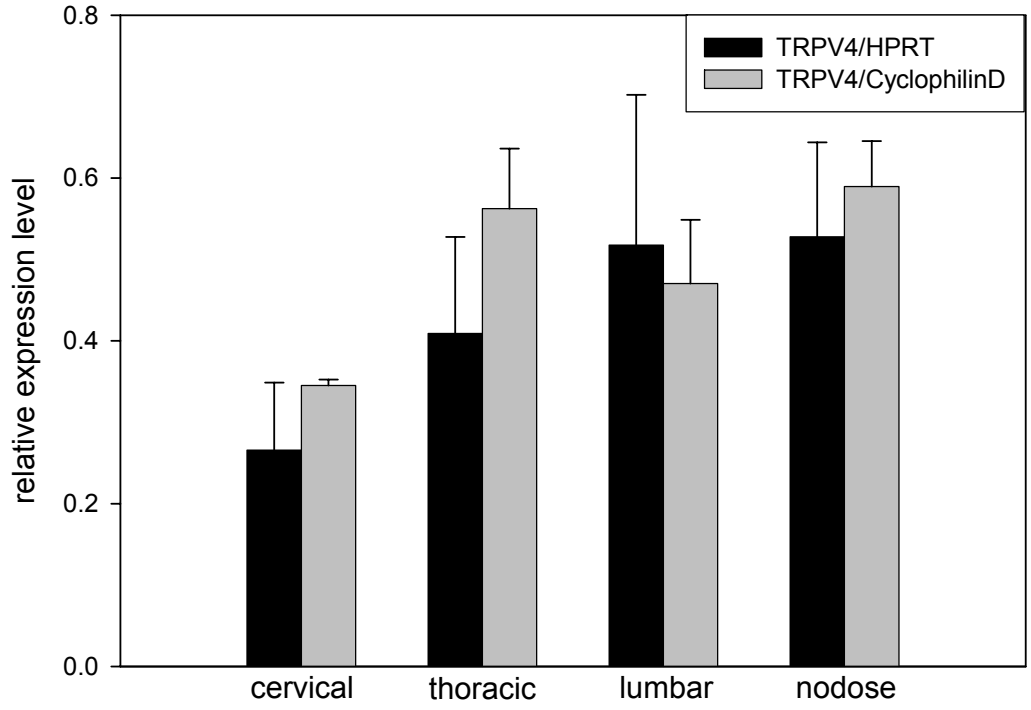

Figure 20: TRPV4 expression in different spinal regions
Real time PCR experiments reveal that TRPV4 is expressed in cervical, thoracic and lumbar DRGs and in the nodose ganglion. TRPV4 expression levels have been normalized against HPRT (black bars) and Cyclophilin D expression levels (gray bars).

3.6.6 Lack of osmosensitivity in small to middle sized DRG neurons in TRPV4 -/- animals

Whole-cell patch clamp studies were conducted on cultured thoracic (T7-T13) DRG neurons twenty four hours after plating. Cultured neurons were kept in isotonic bath solution (310mOsm) and a hypo-osmotic stimulus (260mOsm) was applied using a gravity driven perfusion system. Whole-cell recordings of TRPV4 +/+ neurons revealed a high proportion of cells from the thoracic region to be osmosensitive (67.6%; n=7, 25/37 cells).The population of osmosensitive neurons from TRPV4 -/- mice was significantly decreased (42.1%; n=8, 16/38; $p<0.05$; chi-square test, Figure 21).

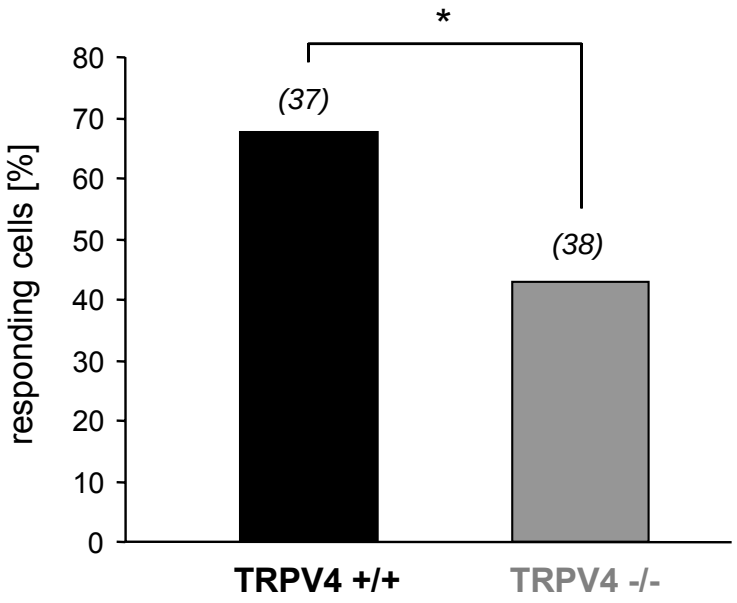

Figure 21: decreased population of osmosensitive cells in TRPV4 -/- DRGs
Whole-cell recordings of thoracic DRG neurons. Cells were challenged for 8s with 260mOsm (bath osmolality: 310mOsm). Responsive cells of TRPV4 +/+ and TRPV4 -/- animals were quantified. Numbers above bars indicate analyzed cells.

It is interesting to note that a population of small to middle-sized cells (cell diameter <30µm) appear to lose their current in TRPV4 -/- neurons. Figure 22A shows a cell size distribution diagram of whole-cell recorded neurons. TRPV4 +/+ and TRPV4 -/- cells were then separated into two subgroups, one containing neurons with a cell diameter smaller and the other greater than 30µm (Figure 22B). When comparing the TRPV4 +/+ and TRPV4 -/- subgroups with a cell diameter <30µm there is a highly significant difference in the number of neurons responding to an osmotic stimulus (68.4%, 13/19 cells and 21.1%, 4/19 cells respectively, $p<0.01$, chi-square test). However, there is no difference in the number of responding neurons when both subgroups with a cell diameter >30µm were compared (66.7%, 12/18 cells and 63.2%, 12/19 cells respectively). There was also no difference in the number of responding cells between TRPV4 +/+ cells with a diameter <30 µm and >30 µm.

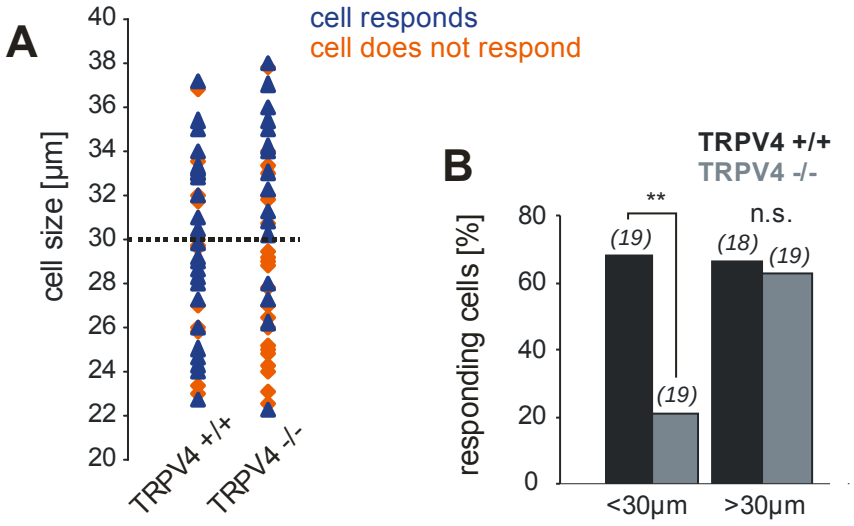

Figure 22: Small to middle sized cells loose their osmosensing ability in TRPV4 -/- DRGs
A, diagram shows the cell size distribution from whole-cell recordings of thoracic DRG neurons from TRPV4 +/+ and TRPV4 -/- animals. Neurons responding to an 8s duration 260mOsm stimulus are marked blue, non-responding neurons are marked orange. **B**, quantification of whole-cell recordings dividing neurons into two groups depending on their size: cells with a diameter smaller than 30µm ($p<0.01$) and those with a diameter greater than 30µm. Numbers above bars indicate analyzed cells.

3.6.7 Characterization of the osmotically evoked current

Sensory neurons can be classified into two groups by the characteristic appearance of their action potential (AP) configuration (Koerber, Druzinsky et al. 1988; Djouhri, Bleazard et al. 1998). Mechanoreceptors with myelinated axons are characterized by very narrow APs whereas small- to medium-sized nociceptors are characterized by wider APs that show a shoulder or 'hump'-like appearance on the falling phase (see Figure 23A). In the previous chapter (3.6.6 and Figure 22) it was demonstrated that small- to middle-sized neurons lose their osmotic current after TRPV4 gene deletion. To see whether it is a particular population of sensory neurons which lose their current the AP appearance of the responding neurons from TRPV4 +/+ and

TRPV4 -/- animals was analyzed and quantified (Figure 23B). In neurons from TRPV4 +/+ mice 55.6% (n=6, 10/18 cells) of the cells that responded to hypotonic stimulation had humped APs. This proportion of neurons was not significantly different compared to the respective proportion found in neurons from TRPV4 -/- mice (50.0%; n=6, 6/12 cells; chi-square test).

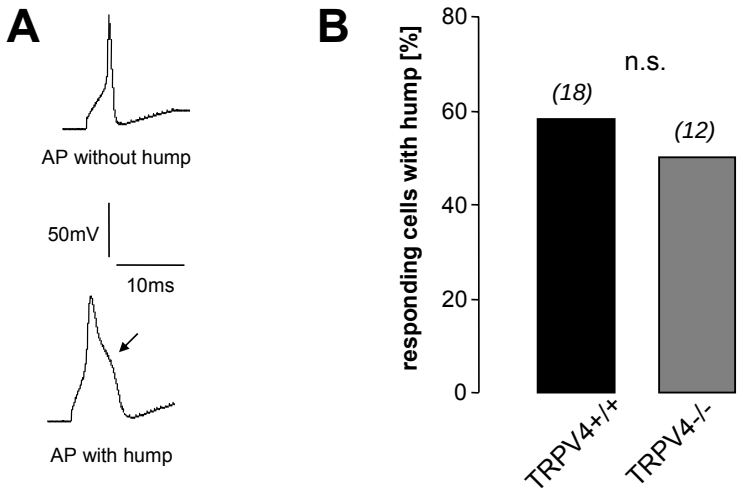

Figure 23: AP analysis of responding cells
A, examples of a narrow AP without hump and a wider humped AP (bottom, arrow indicates the hump). **B**, humped AP quantification of neurons responding with an inward current when stimulated with 260mOsm for 8s. Numbers above bars indicate analyzed cells.

We observed variations of the osmotically evoked current concerning activation and inactivation times when neurons were challenged with hypotonic solutions. Some neurons displayed a rapid inward current (Figure 24A top current trace) while other neurons showed a slowly activating inward current that increased in amplitude for the duration of the stimulus (Figure 24A lower current trace). Furthermore, some currents inactivated rapidly while other currents showed a slow inactivation time (Figure 24A). However, in-depth analysis showed that these currents are actually homogeneous and currents from TRPV4 +/+ neurons are not different compared to currents from TRPV4 -/- neurons in terms of both activation and inactivation times. The top graph in Figure 24B shows a histogram of the activation time

constant tau and the top graph in Figure 24C shows the histogram of the inactivation time constant tau for current traces of TRPV4 +/+ and TRPV4 -/- neurons, both activation and inactivation time constants have been binned (bin width: 0.2s). Both histograms are normally distributed (normality test, p>0.05). The mean activation time of inward currents of neurons from TRPV4 +/+ mice of 0.42 +/- 0.09s (Figure 24B lower graph, 21 analyzed cells, n=6) is not significantly different compared to neurons from TRPV4 -/- mice (0.50 +/- 0.06s; 14 analyzed cells, n=4, t-test). There was also no significant difference in the mean inactivation time as shown in the lower graph of Figure 24C (TRPV4 +/+: 0.51 +/- 0.08s, 25 analyzed cells, n=6; TRPV4 -/-: 0.59 +/- 0.07s, 15 analyzed cells, n=4; t-test). Therefore, none of the observed types of currents appear to be specifically attributable to TRPV4.

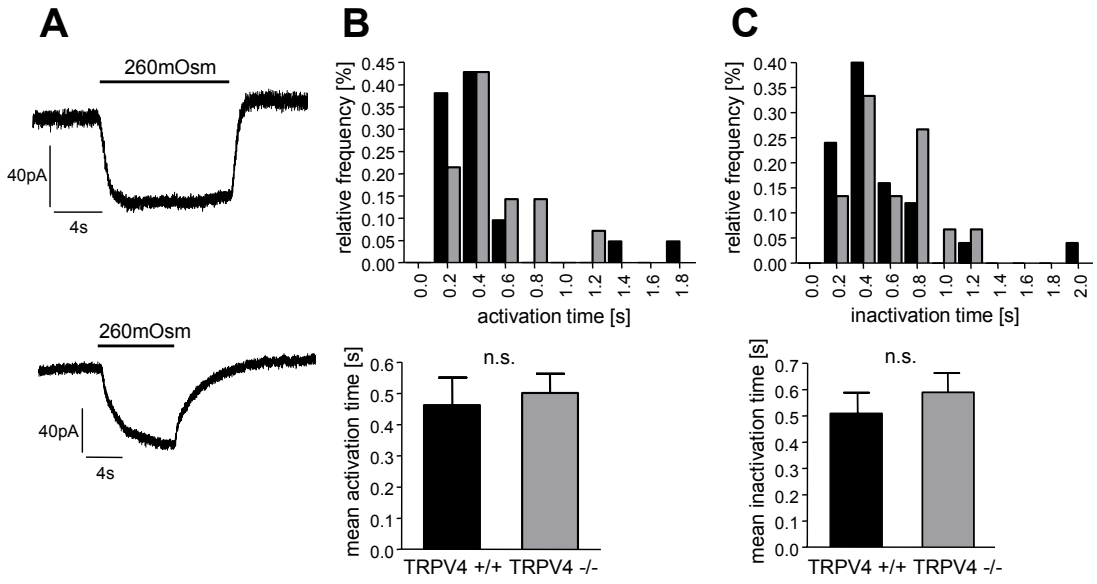

Figure 24: activation and inactivation times of inward currents
A, top trace shows a current with short activation and inactivation time, lower trace shows a current with long activation and inactivation time following hypotonic stimulation (260mOsm). **B**, top graph: histogram of the activation time constant tau for current traces of TRPV4 +/+ and TRPV4 -/- neurons. The activation time constants are binned with a bin width of 0.2s. Lower graph: mean activation time of inward currents from TRPV4 +/+ and TRPV4 -/- neurons. **C**, top graph: histogram of the inactivation time constant tau for current traces of TRPV4 +/+ and TRPV4 -/- neurons. The inactivation time constants are binned with a bin width of 0.2s. Lower graph: mean inactivation time of inward currents from TRPV4 +/+ and TRPV4 -/- neurons.

Furthermore, the osmosensitive current was not blocked by 10µm RR (Figure 25). Figure 25A shows an example trace in which the 260mOsm stimulus before, during and after RR application evokes an inward current of the same size. Amplitudes were normalized to the amplitude of the control stimulus and quantified showing RR does not block the osmotic current (amplitude during 10µm RR stimulation: 96.2 +/- 20.4% of control, wash: 102.4 +/- 17.8% of control, 12 analyzed cells, t-test). In Figure 19 we showed, that RR blocks the Ca^{2+}-responses of thoracic neurons. The finding, that the osmosensitive current is not blocked by RR suggests that the Ca^{2+}-response seen with hypotonic stimuli might occur secondarily to the activation of this current.

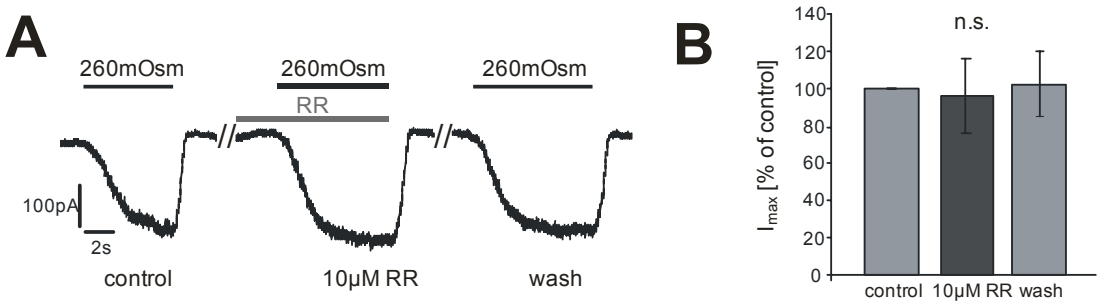

Figure 25: the osmosensitive current is not blocked by RR
A, current trace for control hypo-osmotic stimulus (260mOsm), stimulation in the presence of 10µm RR and stimulation after wash-out of RR. **B**, quantification of the RR block, bars express the maximum amplitude normalized against the control stimulus

3.6.8 Retrograde tracer studies reveal a high osmosensitivity of hepatic afferents, which is absent in TRPV4 -/- mice

To prove that sensory neurons innervating the hepatic system are responsible for peripheral osmoreception a culture system was required that allows one to distinguish between neurons that innervate the liver from those that do not. To achieve this a retrograde tracer (Dextranamin, MW 3000, Molecular Probe) coupled to a fluorophor (Alexa Fluor 488, Molecular Probe) was injected intrahepatically in anesthesized mice. The tracer is taken up by the sensory endings of liver-innervating neurons, transported retrogradely to their cell bodies in the DRGs and thus specifically marks these cells. Optimal labelling occurred 3-4 days post injection and liver-innervating neurons in a thoracic (T7-T13) DRG cell culture could be visualized (Figure 26B, right column). As a control for unspecific staining due to possible dye leakage from the injection site DRG neurons from non-liver-innervating regions (cervical and lumbar) were cultured, but none of these cells were labelled by the tracer (data not shown). A striking proportion of 91.3% (n=7, 21/23 cells; green bar in Figure 26A) of retrogradely labelled neurons responded to a hypotonic stimulus of 260mOsm, a proportion that is significantly higher than found in the entire population of T7-T13 neurons (black bar, $p<0.05$, chi-square test). Thus among the thoracic DRG neurons the population of osmosensitive cells is enriched among those neurons which innervate the liver. The high proportion of osmosensitive cells is absent in retrogradely labelled TRPV4 -/- cells, where only 31.6% (n=4, 6/19 cells) of the cells responded to an osmotic stimulus. The proportion of responding cells is not significantly different comparing retrogradely labelled TRPV4 -/- cells with the entire population of TRPV4 -/- cells. Figure 26B (left column) shows traces of osmotically evoked responses of labelled cells. There were no neurons responding to the 260mOsm stimulus in cultures of retrogradely labelled cells of the nodose ganglion (n=5, 0/16 cells). These results imply that hepatic osmosensation is achieved through sensory DRGs and not by vagal afferents. Furthermore, TRPV4 appears to be essential for hepatic osmosensensing.

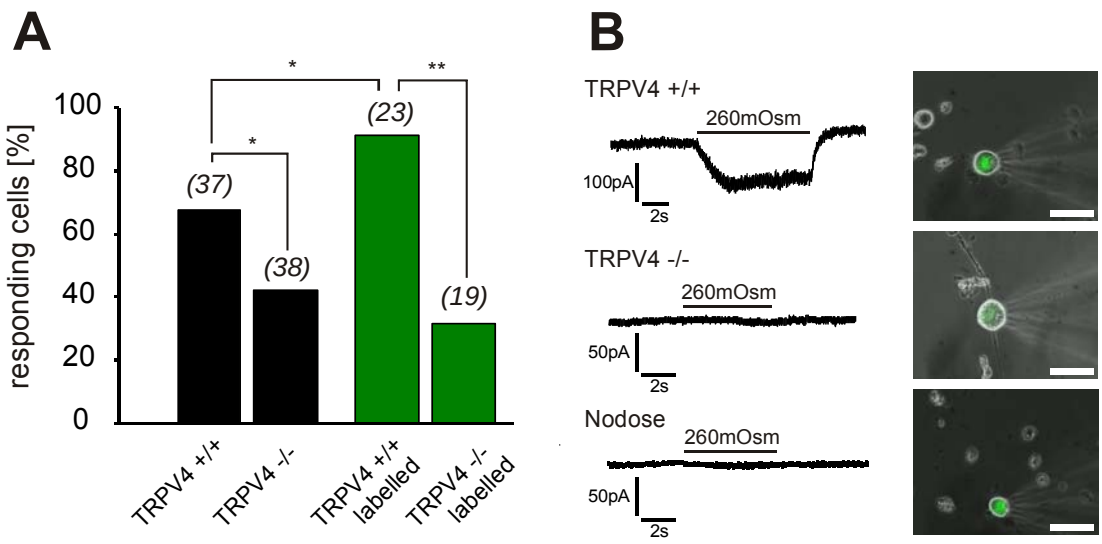

Figure 26: Liver-innervating neurons are highly osmosensitive
A, (left two bars) quantification of whole-cell recordings from thoracic DRG neurons of TRPV4 +/+ and TRPV4 -/- mice. (right two bars) quantification of whole-cell recordings from retrogradely labelled thoracic DRG neurons of TRPV4 +/+ and TRPV4 -/- mice. All cells were challenged with 260mOsm for 8s (bath osmolality: 310mOsm). Numbers above bar indicate analyzed cells. **B**, (left) example traces of retrogradely labelled thoracic DRG neurons of TRPV4 +/+ and TRPV4 -/- mice and of cells from nodose ganglia of TRPV4 +/+ mice. (right) fluorescence micrographs of retrogradely labelled neurons. Scale bar: 50µm.

3.7 Summary

Water-drinking experiments revealed that the increase in ERK activation in hepatic afferents can be significantly inhibited when a TRP-channel blocker (RR) is administered suggesting the involvement of a TRP-channel. TRPV4 -/- animals were intensively studied to unravel the role of TRPV4 in osmosensation. TRPV4 -/- mice are hyperosmolar compared to TRPV4 +/+ animals and *in vivo* experiments demonstrated that ERK phosphorylation does not increase in TRPV4 -/- animals following water administration. Furthermore there is a significant decrease in the proportion of osmosensitive thoracic DRG neurons. In TRPV4 +/+ cells the osmotically evoked Ca^{2+}-response could be inhibited by non-selective TRP-channel inhibitors. Whole-cell patch clamp recordings revealed a significant loss of osmosensitive neurons in TRPV4 -/- mice and this loss only occurs in cells with a diameter smaller than 30µm. There was no significant difference found between the populations of osmosensitive neurons from TRPV4 +/+ and TRPV4 -/- mice regarding the type of cell (AP configuration) or current characteristics. Retrograde labelling experiments revealed that neurons innervating the liver are highly osmosensitive: a striking proportion of over 90% of the neurons has been found osmosensitive. This high proportion is absent in TRPV4 -/- animals. Therefore, liver innervating neurons appear to play a crucial role in peripheral osmosensation and TRPV4 seems to be necessary for peripheral osmoreception.

3.8 The α3nAChR-EGFP-mouse model

3.8.1 EGFP-positive fibers innervate the liver

α3nAChR-EGFP-mice were obtained from GenSat and are a kind gift from Dr. Ines Ibanez-Thallon (MDC, Berlin-Buch). In these animals a 202 kb bacterial artificial chromosome (BAC) has been inserted (Figure 27). The promotor of the α3 subunit of the nicotinic acetylcholine receptor (nAChR) drives expression of the enhanced green fluorescence protein (EGFP).

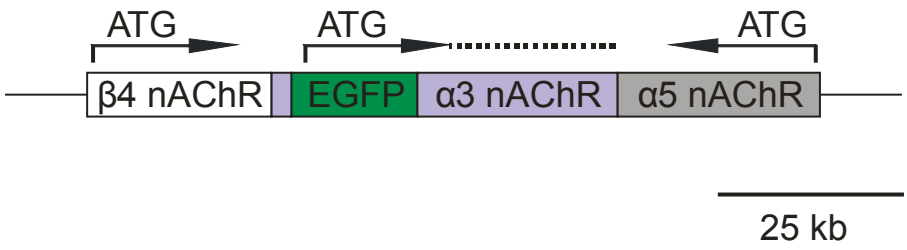

Figure 27: The EGFP-construct
Illustration of the BAC-construct (BAC #RP23-336O6, from GenSat). The construct is 202kb large.

Because of the BAC insertion neurons expressing the α3 subunit of the nAChR also express the reporter EGFP and therefore these neurons can be visualized with fluorescence microscopy. Preliminary studies by the group of Dr. Ines Ibanez-Thallon revealed a robust innervation of the visceral area by EGFP-fibers. To test if α3nAChR-EGFP-mice are a model suitable for studies on osmosensing the population of EGFP-positive neurons was characterized to determine if it is functionally different in terms of osmosensitivity and if they innervate organs involved in peripheral osmosensation. If that is the case then α3nAChR-EGFP-mice might prove suitable for studying peripheral osmoreception. To assess whether the liver is innervated by EGFP-positive

afferents, liver sections of α3nAChR-EGFP-mice were analyzed. Confocal fluorescence microscopy revealed EGFP staining of the surroundings of hepatic blood vessels (Figure 28 top left image). Immunostaining with the neuronal marker PGP9.5 showed colocalization with EGFP-positive fibers thereby confirming their neuronal nature (Figure 28 top row). If the EGFP-positive subpopulation of hepatic neurons is osmosensitive then ERK should be phsphorylated and thereby activated following water-drinking. 8-12 week old α3nAChR mice were given 1ml of water orally and were perfused and fixed twenty minutes later, following which the liver was removed and sectioned. As shown in Figure 28 (lower row) immunostaining revealed that EGFP-positive neurons do indeed show pERK expression.

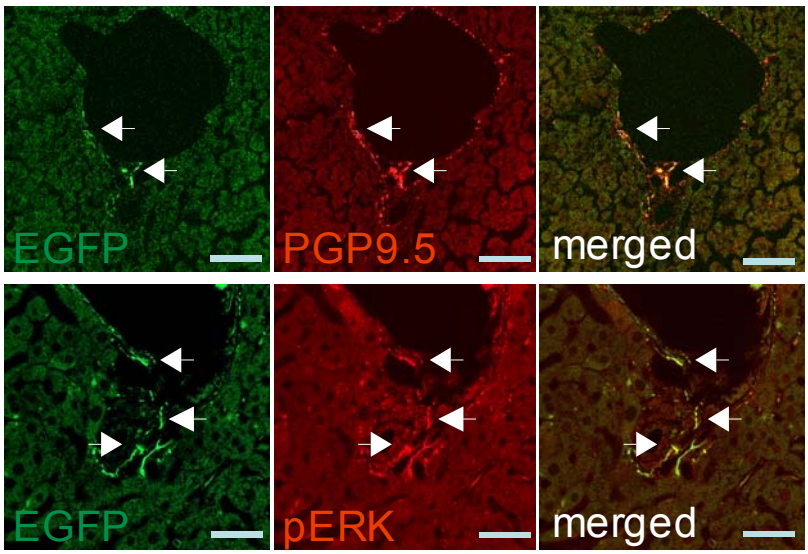

Figure 28: EGFP fibers are pERK positive after water intake
Confocal fluorescence micrographs of liver blood vessels. Upper three images show colocalization of EGFP-positive neurons with the neuronal marker PGP9.5. Lower three images show colocalization of EGFP-positive neurons with pERK. Arrows indicate stained neuronal fibers. Scale bar: 50µm.

3.8.2 EGFP-positive DRG neurons are more osmosensitive

To test whether the population of EGFP-positive neurons is functionally different from EGFP-negative cells in terms of osmosensitivity Ca^{2+}-imaging experiments were conducted. Figure 29A demonstrates the visualization of Fura-2 loaded EGFP neurons. The experimental setup was the same as described in chapter 3.4.1 Briefly twenty four hours after plating thoracic (T7-T13) cells were Fura-2 loaded and kept in 310mOsm bath solution. Hypotonic stimuli of 230mOsm were applied for 22s with a gravity driven multi-barrel perfusion system. Among the entire population of cells (EGFP-positive and -negative together) a proportion of 28.6% (n=4, 62/217 cells) was found to be osmosensitive (Figure 29B black bar). This proportion of thoracic osmosensitive cells in α3nAChR-EGFP-mice is not significantly different from the respective proportion in C57BL/6N mice (30.9%, n=8, 51/165 cells, Figure 12B). Among the EGFP-positive cell population a significantly larger proportion was found to respond when osmotically stimulated (53.2%; n=4, 41/77 cells; $p<0.01$). Among neurons without EGFP-staining the proportion of osmosensitive cells was significantly lower compared to EGFP-positive cells (15%; n=4, 21/140 cells; $p<0.01$), the proportion was even significantly decreased when compared to the entire population of cells ($p<0.05$, all statistics done with chi-square test).

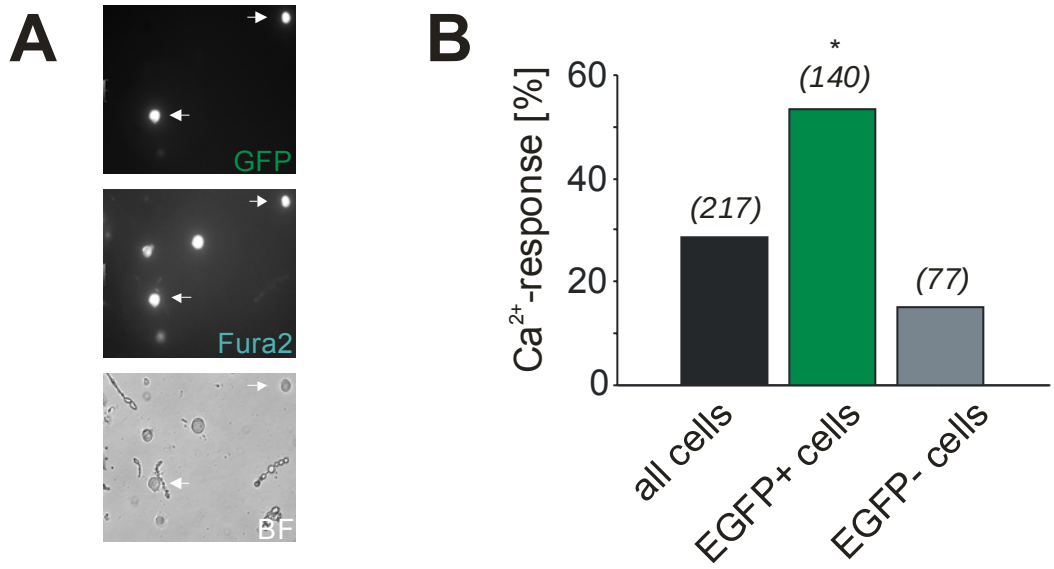

Figure 29: More EGFP cells are osmosensitive
A, bright field (BF) and fluorescence Fura-2 (380nm) and GFP (488nm) images of the same cells of thoracic DRG neurons from α3nAChR-EGFP mice. Arrows indicate EGFP-positive cells. **B**, quantification of the Ca^{2+}-responses of thoracic DRG neurons from α3nAChR-EGFP mice mice to a hypo-osmotic 230mOsm stimulus. Numbers above bars indicate analyzed cells.

3.9 Summary

EGFP-positive neurons could be visualized to innervate the liver and they show ERK-activation following water-drinking. Furthermore, Ca^{2+}-imaging experiments demonstrated that osmosensitive neurons are enriched in the EGFP-positive population of cells. The combination of *in vivo* ERK-immunostaining and Ca^{2+}-imaging experiments show for the first time that the cell body located in thoracic DRGs as well as the afferents located in the liver both respond following hypotonic stimulation. Thus, the α3nAChR-EGFP-mouse appears to be suitable for further studies of osmosensation providing a model in which the neurons of interest can easily be visualised without any preceding marking experiments.

4 Discussion

The cells of the body are surrounded by an extracellular fluid (ECF) which supplies ions and nutrients for the cells. The ECF osmolality is a measure of the concentration of these substances and is kept at a highly stable set-point (Bourque 2008). Changes in ECF osmolality can affect cell integrity, metabolism and function and under extreme conditions can have traumatic or lethal consequences (Steenbergen, Hill et al. 1985; Somero 1986; Cserr, DePasquale et al. 1987; Gullans and Verbalis 1993; Verbalis 2003). Therefore, a divergence towards either hypotonicity or hypertonicity triggers behavioral and humoral responses to keep ECF osmolality close to the set-point (Sharif-Naeini, Ciura et al. 2008). The tight regulation of ECF osmolality implies the existence of a sensory system able to detect changes in osmolality. Osmoreceptors have been found both centrally and peripherally. Central osmoreceptors were first described in 1947 (Verney 1947) and until today they have been studied the most extensively. They are located in the circumventricular organs, which are brain regions with a weak or non-existent blood brain barrier (Buggy and Jonhson 1977; McKinley, Denton et al. 1982; Thrasher, Keil et al. 1982). Further studies suggested the following brain regions to be responsible for central control of osmoregulation: the subfornical organ (SFO), the median preoptic nucleus (MnPO) and the organum vasculosum lamina terminalis (OVLT) (Gutman, Ciriello et al. 1988; Honda, Negoro et al. 1990). The osmosensitivity of neurons in the MnPO and OVLT has been shown employing electrophysiological experiments (Richard and Bourque 1994; Ciura and Bourque 2006).

Peripheral osmoreceptors have received much less attention and their exact location remains unknown. Several studies showed the existence of peripheral osmoreceptors indirectly. They reported behavioral and humoral responses were triggered shortly after osmotic stimulation at a time point where systemic ECF osmolality is still unchanged and therefore a regulatory response by central osmoreceptors could be excluded (Haberich 1968; Baertschi and Pence 1995; Carlson, Beitz et al. 1997; Stricker and Hoffmann

2007). This means peripheral osmoreceptors can detect changes in osmolality due to ingested food or fluid well before central osmoreceptors are able to do so. Therefore they can induce anticipatory responses through afferent connections to the CNS and buffer the potential impact that consumption related osmotic changes might have.

This study is concerned with the anatomical and physiological characterization of peripheral osmoreceptors. A large part of this study is concerned with the investigation of a mutant mouse model, in which the *TRPV4* gene has been disrupted to unravel the role of the non-selective cation channel TRPV4 in peripheral osmosensing.

4.1 Peripheral osmoreception

4.1.1 Osmosensation of spinal liver innervating neurons

Direct measurements of the portal vein blood osmolality in mice revealed that drinking 1ml of water leads to a decrease of portal vein blood osmolality by approximately 25mOsm from 310mOsm to 285mOsm within thirty minutes (Figure 8). This was the physiological stimulus for hepatic peripheral osmoreceptors applied in all further *in vivo* water-drinking experiments. Liver innervating peripheral afferents able to detect hypotonic changes in osmolality should thus have a sensitivity in this physiological range (310-285mOsm, Figure 8). We established an *in vivo* animal model for detection of osmotic nerve stimulation based on the activation of the extracellular-signal regulated kinases 1 and 2 (ERK 1/2). As described in chapter 3.2 ERK activation occurs not only to osmotic stimuli but also to various other stimuli. Therefore two controls (sham and PBS administration) were included to exclude non-osmotic effects and it was shown, that water-drinking leads to a significant increase in ERK activation in neurons innervating hepatic blood vessels (Figure 10). Hepatic innervation is achieved through DRG axons whose cell bodies are located in the thoracic region of the spinal cord (Magni

and Carobi 1983; Berthoud 2004). By employing Ca^{2+}-imaging experiments it was shown for the first time, that there is a significantly higher proportion of osmosensitive neurons in thoracic DRGs (approximately 30%) compared to neurons from the cervical or lumbar regions (both approximately 10%, Figure 12). One other study conducted Ca^{2+}-imaging experiments on cultured DRG neurons from the lumbar region and analyzed their response to hypotonic stimuli, but the authors neither mentioned the percentage of neurons responding to the stimulus nor did they conduct a comparison to DRG neurons from other spinal regions (Alessandri-Haber, Dina et al. 2006). Whole-cell electrophysiological recordings of thoracic neurons revealed a very high proportion (approximately 68%) of the cells to be osmosensitive (Figure 21). Until now, there was no direct evidence showing osmosensation of spinal afferents innervating the liver. Our *in vivo* water-drinking experiments did show that there are hepatic neurons, which are activated when osmotically stimulated, but these experiments did not show where these neurons originate. Our calcium-imaging and patch clamp studies revealed a high proportion of osmosensitive neurons in the thoracic region. It is known that the liver is innervated by afferents from DRGs located in the spinal thoracic region (Magni and Carobi 1983; Berthoud 2004), but we do not know whether the axons of the neurons from the osmosensitive population innervate the liver. At the starting point of this study there were no reports showing direct evidence of hepatic osmoreception. One study reported that osmotically evoked signalling to the hypothalamo-neurohypophysial system can be abolished by injection of a local anaesthetic into the thoracic region of the spinal cord (Vallet and Baertschi 1982). This experimental result supports the essential role of DRGs from this region in osmosensation, but the location of the endings of these neurons, where the actual osmoreception takes place, remained unknown. To investigate specifically the function of liver-innervating neurons in terms of osmoreception we combined retrograde labelling techniques with whole-cell patch clamp recording experiments. The retrograde tracer was injected intrahepatically in anesthetized mice, is taken up by the sensory endings of liver-innervating neurons, transported retrogradely to their cell bodies in

thoracic DRGs and specifically marks these cells. Thus, this model allows one to distinguish between liver-innervating neurons and those that do not innervate the liver within a cell culture of thoracic DRGs. A striking proportion of 91% of retrogradely labelled neurons responded with an inward current when challenged with hypotonic solution (Figure 26), which is the first direct evidence demonstrating a proportion of osmosensitive liver-innervating neurons. This proportion is even significantly higher than the proportion of osmosensitive cells found in the entire population of thoracic neurons (67%). Thus among the thoracic DRG neurons the population of osmosensitive cells is enriched among those neurons that innervate the liver.

In primary cell culture systems one separates the neuron somata from their tissue-innervating axonal endings. Therefore, in calcium-imaging and whole-cell patch clamp experiments of cultured neurons one applies a stimulus to the somata of the cells and measures the response of the cell somata and not of the neuronal endings, as this is not possible in cell culture. One usually assumes that the neuronal sensory endings of the cell display the same response as the somata, but one cannot be certain that the responsiveness of somata and sensory endings are indeed identical.

We had access to the α3nAChR-EGFP-mouse model, which allowed us to analyze the osmosensitivity of cultured neurons as well as the afferent endings of these cells in the liver. In these animals a 202 kb BAC has been inserted (Figure 27). The promotor of the α3 subunit of the nAChR drives expression of EGFP. Thus, neurons expressing the α3 subunit of the nAChR also express the reporter EGFP and therefore these neurons can be visualized with fluorescence microscopy. Preliminary studies by the group of Dr. Ines Ibanez-Thallon revealed a robust innervation of the visceral area by EGFP-fibers.

In *in vivo* experiments EGFP-positive fibers were found to innervate the liver and confocal fluorescence microscopy showed that ERK becomes activated in these neurons following water-drinking of the animal (Figure 28). Figure 29 demonstrates that among the EGFP-positive population of cultured thoracic DRG neurons a significantly larger proportion was found to be osmosensitive

(53%) compared to neurons without EGFP-staining (15%) by employing the Ca^{2+}-imaging technique. Our results proved this model to be suitable for future research on osmosensing offering the following advantages: This model allows one not only to observe and analyze osmosensitive neurons in cell culture systems, but one can actually analyse the afferent endings of these cells within the innervated tissue. Additionally, experiments can be carried out without a preceding complicated marking procedure for visualization of osmosensitive neurons due to the EGFP-staining. In contrast, it is important to note that these results are based on analysis of liver-innervating afferents and neurons from thoracic T7-T13 DRGs only and may not be generalized on EGFP-positive fibers innervating other tissues with somata in other spinal DRGs.

In conclusion our data suggests that water-drinking leads to a spinal reflex involving a subpopulation of highly osmosenssitive thoracic DRG neurons whose axons terminate in the liver.

4.1.2 Vagal afferents and peripheral osmosensation

The vagus nerve is the main nerve providing parasympathetic innervation of the upper abdominal organs including the liver. The cell somata of vagal afferent neurons are located in the nodose ganglia (Magni and Carobi 1983; Berthoud, Kressel et al. 1992). Some studies have reported a contribution of vagal afferents from the nodose ganglia in osmoreception. One study demonstrated vagal activity upon peripheral osmotic stimulation (Mei and Garnier 1986). The authors recorded the activity of sensory vagal neurons with extracellular glass microelectrodes implanted in the nodose ganglia in anesthetized cats. The nodose neurons were activated by perfusion of the small intestine with tap water as hypotonic stimulus and various hypertonic solutions (the osmolality of the solutions ranged between 4 and 1100mOsm). In general, the authors found that hypotonic solutions and tap water induced the more marked responses. The study demonstrates the contribution of the vagal system in osmoreception, but does not address the specific location of

where vagal osmoreception takes place. Another study investigated the contribution of the hepatic and portal vein area to vagal osmoreception (Adachi, Niijima et al. 1976; Adachi 1984). The authors perfused rat liver with hypo- and hypertonic solutions through the portal vein and analyzed vagal neural responses (spike discharges) to changes in osmolality of the perfusion solutions. This study showed that two different types of osmosensitive afferent fibers exist in the hepatic vagus, one was characterized by increasing the frequency of spike discharges responding to hypertonic stimulation, while the other showed the same response to hypotonic stimulation.

In our study we found 10% of neurons from the nodose ganglia responded in Ca^{2+}-imaging experiments when stimulated by hypotonic solution (Figure 12). However, this proportion of responding cells was the same as found in cervical and lumbar spinal regions (11% and 9%, respectively) and is significantly lower compared to thoracic neurons (31%). Still, this result shows that neurons from the nodose ganglia are able to detect osmotic changes, even when the proportion of neurons with this ability is significantly lower than found in thoracic DRGs. To address the question of whether this small population of osmosensitive neurons from nodose ganglia innervates the liver, whole-cell patch clamp recordings on retrogradely labelled nodose neurons were conducted. Out of 16 analyzed neurons not one cell responded to hypotonic stimulation. Nodose neurons received the same stimulus of 260mOsm as thoracic neurons. We do know that the inward current of an osmosensitive cell increases with the hypotonicity of the stimulus (see Figure 15) and 260mOsm is a relatively large stimulus to which osmosensitive neurons should respond. However, as labelled nodose neurons did not respond to this hypotonic stimulus our conclusion was that liver-innervating nodose neurons are likely not involved in peripheral osmoreception.

Retrograde and anterograde tracing studies showed that vagal innervation of the liver is not very dense (Magni and Carobi 1983). Most vagal afferent fibers travelling in the common hepatic branch predominantly innervate tissues immediately adjacent to the liver rather than the liver itself (Magni and Carobi 1983; Berthoud, Kressel et al. 1992). For example, the hepatic artery

and portal vein areas receive dense vagal innervation (Barja and Mathison 1984) suggesting that they are potential candidates for vagal osmosensing. Also the studies by Adachi et al. (Adachi, Niijima et al. 1976; Adachi 1984) on vagal osmosensing upon osmotic perfusion of the portal vein supports the idea of vagal osmosensing in the portal vein.
Taken together out data supports the contribution of vagal afferents to osmoreception, but they do so to a much lesser degree than spinal thoracic afferents. Furthermore our data suggests that vagal osmoreception does not take place in the liver as no liver-innervating osmosensitive nodose neurons were found.

Figure 30 summarizes our findings on peripheral hepatic osmosensing. Conducting whole-cell patch clamp experiments on retrogradely labelled neurons from thoracic DRGs, we found a subpopulation of highly osmosensitive neurons whose axons terminate in the liver (Figure 30A, upper image). Employing the same technique we did not find neurons from nodose ganglia to respond to hypotonicity, suggesting nodose neurons are likely not involved in peripheral vagal osmoreception (Figure 30A, lower image). *In vivo* water-drinking experiments on α3nAChR-EGFP-mice revealed, that ERK becomes activated in EGFP-stained hepatic afferents following water-drinking. Furthermore, Ca^{2+}-imaging of thoracic neurons from α3nAChR-EGFP-mice showed, that these neurons are also more responsive to hypotonic stimuli (Figure 30B).
Our data suggests that water-drinking leads to a spinal reflex involving a subpopulation of thoracic DRG neurons with hepatic afferents, whereas vagal hepatic afferents are likely not involved in hepatic peripheral osmoreception.

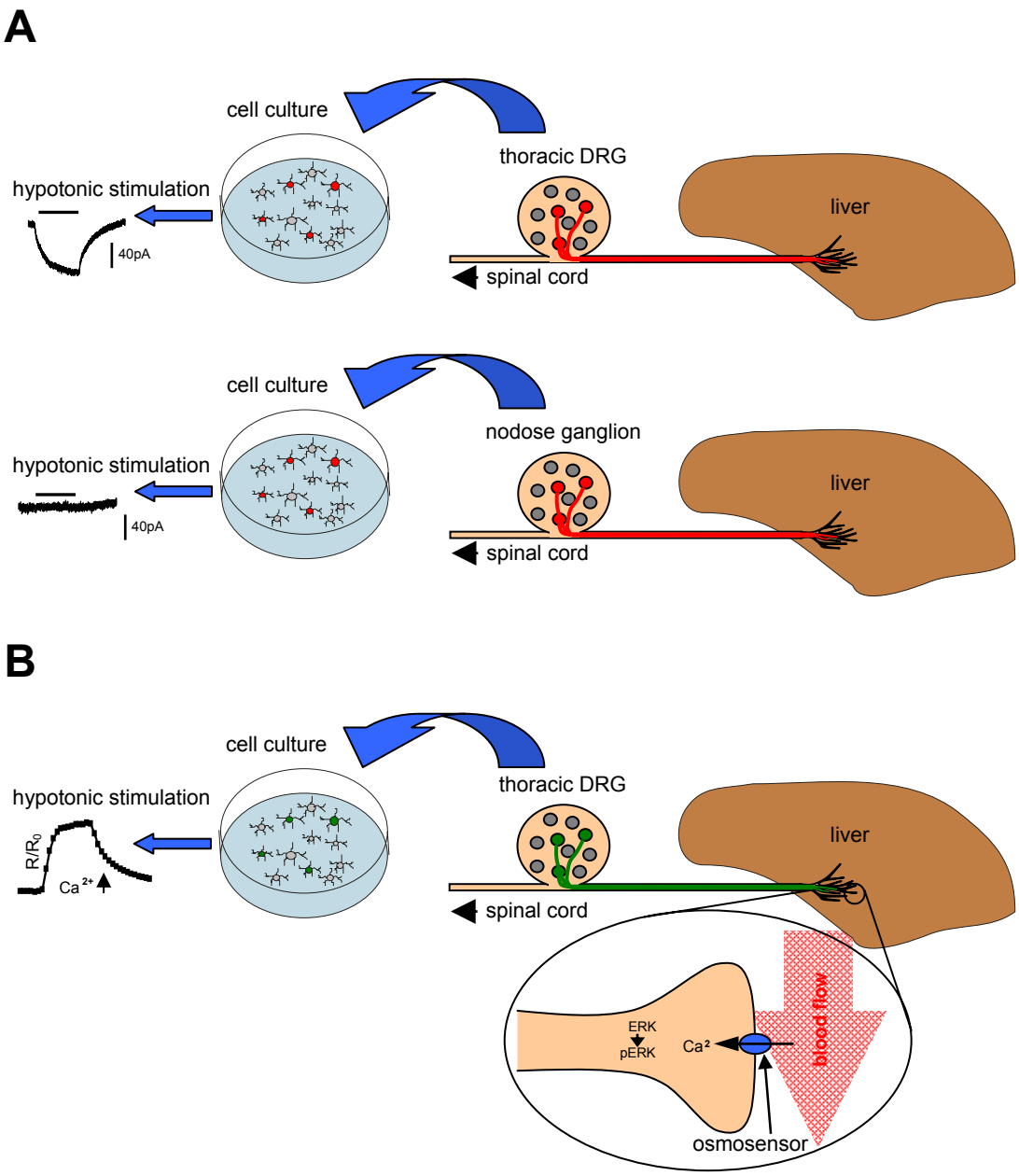

Figure 30: Schema of osmoreception in the liver
A, summary of retrograde labelling experiments. Upper image: The liver is innervated by afferents from thoracic DRG neurons (marked in red). Taken into culture a high proportion of these neurons was found to be osmosensitive. Lower image: Vagal afferents from nodose ganglia innervate the liver (red). However, labelled neurons were not found osmosensitive. **B**, EGFP-neurons innervate the liver (green). ERK becomes activated in these neurons following water-drinking. A high proportion of cultured thoracic EGFP-neurons showed Ca^{2+}-responses to hypotonicity. An osmosensor (blue) located at the sensory endings of thoracic hepatic afferents detects hypotonic changes in blood osmolality and signals to the CNS to induce anticipatory responses.

4.2 The role of TRPV4 in osmoreception

Experiments performed on the nematode worm *Caenorhabditis elegans* indicated the first evidence of a role of a TRPV ion channel member in osmoreception (Colbert, Smith et al. 1997). Worms lacking a functional OSM-9 protein did not show the typical avoidance behavior when confronted with aversive osmotic stimuli and they did not respond to mechanical stimuli applied to the nose. The OSM-9 protein showed homology with the *Drosophila melanogaster* photoreceptor TRP and further research identified TRPV4 as the vertebrate homolog of OSM-9. Thus TRPV4 was the first mammalian TRPV channel reported to be involved in osmoreception (Liedtke, Choe et al. 2000; Strotmann, Harteneck et al. 2000). During the last few years mutant mouse models were generated in which the *TRPV4* gene was disrupted. In the present study we examined the role of TRPV4 using TRPV4 -/- mice.

The portal vein blood osmolality of TRPV4 -/- mice was found to be hyper-osmolar compared to TRPV4 +/+ animals (316mOsm/kg and 310mOsm/kg respectively, Figure 16). This phenotype is consistent with observations made in another study that measured systemic blood osmolality of 300mOsm/kg and 295mOsm/kg respectively (Liedtke and Friedman 2003). *In vivo* experiments revealed that water-drinking leads to a significant increase in ERK activation in neurons innervating hepatic blood vessels of TRPV4 +/+ mice (Figure 10). An increased ERK activation after water-drinking was not found in liver sections from TRPV4 -/- animals (Figure 17). The observed level of phosphorylated ERK was the same in all three tested groups (sham, PBS and water administration) suggesting that hypotonic osmoreception in the liver is impaired in TRPV4 -/- animals. However, because the blood osmolality of TRPV4 -/- mice is hyperosmolar, there is an alternative explanation. The peripheral osmoreceptor might only become activated when the blood osmolality reaches a certain threshold value. Figure 16 shows TRPV4 -/- mice have a higher resting blood osmolality and also shows that the blood osmolality following water-drinking stays constantly higher compared to TRPV4 +/+ mice. Therefore, hepatic osmoreceptors in TRPV4 -

/- mice are not exposed to the same magnitude of hypo-osmolality following water-drinking. Thus, pERK levels may not increase in TRPV4 -/- mice because the threshold value for osmoreceptor activation was not reached.

In a cell culture system the difference in osmolality of the cell environment can be eliminated. In contrast to *in vivo* experiments one can ensure that cultured neurons from both TRPV4 +/+ and TRPV4 -/- mice are surrounded by a bath solution of the same osmolality and receive the same osmotic stimulus during Ca^{2+}-imaging and whole-cell patch clamp experiments. In Ca^{2+}-imaging experiments of cultured thoracic neurons 31% of cells from TRPV4 +/+ mice were found to be osmosensitive. The osmosensitive cell population in TRPV4 -/- mice was significantly lower at just 11% (Figure 18). Whole-cell patch clamp recordings of neurons from thoracic DRGs confirmed this finding: 68% of neurons from TRPV4 +/+ mice responded with an inward current when stimulated with hypotonicity, this proportion was significantly lower in neurons from TRPV4 -/- animals (42%, Figure 21). These findings demonstrate that TRPV4 plays an important role in peripheral osmosensation. To unravel the contribution of TRPV4 in peripheral osmoreception within the hepatic DRG neurons with afferent endings located in the liver were marked by retrograde labelling allowing specific analysis of these neurons. Whole-cell patch clamp recordings of labelled neurons revealed that almost all (91%) were osmosensitive neurons, a proportion that was dramatically reduced to 32% in TRPV4 -/- mice (Figure 26).
Thus it can not only be concluded that TRPV4 plays an essential role in peripheral osmoreception, but TRPV4 seems to be crucial especially for peripheral osmoreception in the liver.

TRPV4 is essential for osmoreception, but the question remains: is TRPV4 the actual osmosensing channel? The proportion of osmosensitive thoracic DRG neurons is significantly reduced in TRPV4 -/- mice, but there is still a substantial number of osmosensitive neurons in TRPV4 -/- mice (Figure 21 and 25). Furthermore, there is a small proportion of osmosensitive neurons in cervical and lumbar DRGs and there is no significant difference in this

population between TRPV4 +/+ and TRPV4 -/- mice (Figure 18). These observations may be explained by the existence of other osmosensitive channels. For example, TRPV1 and TRPV2 have been reported to be osmosensitive as described in chapter 1.5 (Birder, Nakamura et al. 2002; Muraki, Iwata et al. 2003; Ciura and Bourque 2006; Sharif Naeini, Witty et al. 2006) and the remaining osmoreception in TRPV4 -/- mice may be achieved through these channels.

Assuming TRPV4 is an osmosensor then the respective current should disappear in TRPV4 -/- animals, which would be expected to cause a change in current activation and/or inactivation kinetics. In-depth analysis revealed, that the observed currents in sensory neurons from TRPV4 +/+ animals are homogenous and that currents in sensory neurons from TRPV4 -/- animals were not significantly different (Figure 24). Therefore these currents may not be specifically attributable to TRPV4 and it is highly unlikely that TRPV4 alone is responsible for osmoreception in thoracic neurons. It might even be possible, that TRPV4 is indirectly activated by a different channel that senses osmolality. Supporting this idea, we found that the osmotic inward current was not blocked by the TRP-channel blocker RR (Figure 25), but RR inhibits the Ca^{2+}-response following hypotonic stimulation (Figure 19). Thus our data suggests, that TRPV4 at least partly mediates the increase in Ca^{2+} which might occur secondarily to the activation of the osmotic current. This finding is consistent with previous studies which reported, that TRPV4 opens secondarily as a result of the release of lipid products or second messengers (Watanabe, Vriens et al. 2003; Reiter, Kraft et al. 2006)

The osmoreceptor may be a heteromultimeric protein complex formed by different types of TRPV channel subunits. TRPV channel subunits have indeed been shown to heteromerize in heterologeous as well as in native systems (Rutter, Ma et al. 2005; Cheng, Yang et al. 2007) so TRPV4 might be an essential part of a multi-protein complex. Two studies reported that heterologous expression of TRPV4 in CHO and human HEK293 grants these cells the *de novo* ability to respond to hypotonic stimuli measured by fluo-4 AM based Ca^{2+}-imaging (Liedtke, Choe et al. 2000; Strotmann, Harteneck et

al. 2000), fura-2 based Ca^{2+}-imaging and whole-cell patch clamp experiments (Liedtke, Choe et al. 2000; Strotmann, Harteneck et al. 2000). These studies seem to contradict the idea of a multi-component osmosensor and seem to support the idea that TRPV4 alone might be sufficient for osmereception. However, osmosensor subunits might be present in these cells and after TRPV4 transfection a multi-protein complex might render these cells osmosensitive. Therefore data based on heterologeous overexpression of TRPV4 cannot be compared with the analysis of native systems, also Ca^{2+} responses and currents from CHO and HEK293 transfection experiments are not comparable to *in vivo* systems. Using RT-PCR we found that TRPV4 is expressed in all spinal regions and in the nodose ganglia (Figure 20). Although there was no significant difference in the expression levels, a high proportion of osmosensitive cells was only found in neurons from thoracic DRGs (Figure 18, 21 and 26). Therefore TRPV4 may be a crucial part of a multi-protein osmoreceptor complex that transduces osmotic stimuli only within the thoracic region where other proteins required for osmosensing are present and TRPV4 may play a different role in other spinal regions where these proteins are absent. There are many studies which demonstrated that TRPV4 plays a role in other, non-osmoreception related processes. It has been reported that TRPV4 is involved in mechanical pain sensation and hyperalgesia (Alessandri-Haber, Joseph et al. 2005; Alessandri-Haber, Dina et al. 2006) or hyperalgesia especially in the viscera (Brierley, Page et al. 2008; Cenac, Altier et al. 2008). In conclusion, our data provides evidence that TRPV4 is crucial for peripheral osmosensation and that the high proportion of osmosensitive neurons from hepatic thoracic DRGs is attributable to TRPV4. TRPV4 is unlikely to be the osmosensor itself, but may either be activated secondarily following activation of the osmosensor or alternatively TRPV4 may be an essential part of a multi-component osmosensor.

4.3 Activation mechanism

Although this study did not investigate the activation mechanism of the osmosensor, we made an interesting observation concerning the activation mechanism. When a cell is exposed to hypotonicity, water will enter the cytoplasm causing membrane stretch and a subsequent increase in cell volume. Thus it is believed, that osmosensory transduction is mediated by mechanical membrane stretching, which is associated with osmotically evoked change in cell volume (Oliet and Bourque 1993; Zhang and Bourque 2003; Zhang, Kindrat et al. 2007; Bourque 2008). The group of Bourque found that hypo-osmotic stimuli cause hyperpolarization and hyper-osmotic stimuli cause depolarization of MNCs. They demonstrated that during whole-cell patch clamp experiments the decrease in cation conductance associated with cell swelling caused by hypotonic stimulation could be reversed by restoring the cell volume via the application of negative pressure to the recording pipette. The authors concluded that in this case of stretch inactivated channels osmosensory transduction is mediated by membrane stretch.

However, it might also be possible that membrane stretch, while concurring with changes in osmolality, might not be the activation mechanism itself. We observed a discrepancy in the time course of cell swelling following osmotic stimulation and the inward current in separate whole-cell patch clamp experiments. Neurons receiving a hypotonic stimulus increased in cell size approximately one second following osmotic stimulation reaching their maximum size after 8-9 seconds (Figure 13). We do not know the exact onset of the change in cell size in magnitudes of miliseconds because a sampling frequency of one hertz was used. In whole-cell patch clamp experiments we calculated a mean activation time constant tau of 0.42 +/- 0.09s (Figure 24). Due to the rapid activation time of hypotonically evoked currents and a relatively slow increase in cell size it might be possible, that the osmosensor senses osmolality changes directly by an as yet unknown mechanism. Further experiments are necessary to investigate the possible role of cell swelling as activation mechanism. In particular, whole-cell patch

clamp experiments should be combined with cell size measurements during osmotic stimulation of neurons to unravel whether the currents appear during or at a time point before changes in cell size.

4.4 Conclusions

- Water-drinking is a spinal reflex and leads to an activation of hepatic afferents. Peripheral osmoreception is achieved by a subpopulation of highly osmosensitive thoracic neurons whose axons innervate the liver.
- Peripheral osmoreception is achieved through a spinal reflex rather than through vagal afferents. Vagal afferents do not contribute to hepatic osmoreception.
- Studies with TRPV4 -/- mice revealed that TRPV4 is essential for peripheral osmosensation. TRPV4 is crucial for osmoreception by neurons from hepatically innervating thoracic DRGs. TRPV4 alone may not be the osmosensor, but may be activated secondarily by the osmosensor or TRPV4 may be an essential component in a multi-protein osmosensor.
- *In vivo* ERK-immunostaining and Ca^{2+}-imaging experiments on EGFP-positive neurons of the α3nAChR-EGFP-mouse showed that the cell body located in thoracic DRGs as well as the liver innervating afferents both respond to hypotonic stimulation. Thus, the α3nAChR-EGFP-mouse offers an interesting animal model for studies on osmosensation.

5 Summary

The extracellular fluid surrounds our cells and supplies them with ions and nutrients. Changes in extracellular fluid osmolality can affect cell integrity, metabolism and function and under extreme conditions can have lethal consequences. Therefore, our body strives to keep extracellular fluid osmolality at a highly stable set-point and a divergence towards either hypotonicity or hypertonicity triggers behavioral and humoral responses. The underlying mechanism for detection of changes in osmolality is called osmoreception. Osmoreceptors have been found both centrally and peripherally. Whereas central osmoreceptors have been well studied, peripheral osmoreceptors have received much less attention. This study is concerned with the analysis of the effect of water-drinking and investigates the role of the sensory innervation of the liver in peripheral osmoreception. Furthermore, the role of the ion channel TRPV4, which has been shown to be involved in osmoreception, is studied.

The physiological stimulus for water-drinking in mice has been assessed. To investigate activation of peripheral afferents due to water-drinking, an animal model based on pERK immunostaining has been developed. We observed an increase in ERK activation in hepatic neurons innervating liver blood vessels following water-drinking, which indicated an involvement of the liver in peripheral osmoreception. Employing Ca^{2+}-imaging and whole-cell patch clamp experiments we studied the osmosensitivity of DRG neurons from cervical, thoracic and lumbar spinal regions. Thoracic neurons displayed a significantly higher proportion of osmosensitive cells compared to neurons from other spinal regions. By using a retrograde tracer injected in the liver, we could visualize the liver innervating population of thoracic DRG neurons and found a strikingly high proportion of cells from this population to be osmosensitive. Thus, we could show the involvement of the liver in peripheral osmoreception. Further whole-cell patch clamp experiments demonstrated, that indeed thoracic DRG neurons and not vagal neurons of the nodose ganglia transduce hepatic osmotic stimuli.

A large part of this study was concerned with the analysis of TRPV4 -/- mice. It was found, that upon deletion of the TRPV4 gene, water-drinking did not increase pERK levels in hepatic afferents. The population of osmosensitive thoracic DRG neurons from TRPV4 -/- mice was found to be significantly decreased as shown with Ca^{2+} imaging and whole-cell patch clamp experiments. These results indicated a crucial role of TRPV4 in peripheral osmoreception.

Zusammenfassung

Die Extrazellulärflüssigkeit umgibt unsere Zellen und versorgt sie mit Ionen und Nährstoffen. Eine Änderung der Osmolalität der Extrazellalärflüssigkeit kann Auswirkungen auf die Integrität von Zellen, ihren Metabolismus und ihre Funktion haben und unter extremen Bedingungen kann sie sogar letale Konsequenzen haben. Deshalb ist unser Körper sehr bestrebt, die Osmolalität der Extrazellalärflüssigkeit um einem stabilen Sollwert zu halten. Hypo- und hypertone Abweichungen der Osmolalität vom Sollwert löst hormonale- und verhaltensspezifische Reaktionen aus, die die Osmolalität zurück zum Sollwert regulieren. Der zugrundeliegende Mechanismus zur Detektion von Veränderungen der Osmolalität heisst Osmorezeption. Osmorezeptoren wurden sowohl im zentralen als auch im peripheren Nervensystem gefunden. Zentrale Osmorezeptoren wurden schon relativ gut studiert, wohingegen peripheren Osmorezeptoren wesentlich weniger Aufmerksamkeit geschenkt wurde. Diese Arbeit beschäftigt sich mit der Analyse des Effekts von Wassertrinken und untersucht insbesondere die Rolle der sensorischen Innervation der Leber in peripherer Osmorezeption. Weiterhin wird die Rolle des TRPV4 Ionenkanals untersucht, von dem bekannt ist, dass er an Osmorezeptionsprozessen beteiligt ist.

Der physiologische Stimulus des Wassertrinkens wurde gemessen. Um die Aktivierung peripherer Afferenzen durch Wassertrinken zu untersuchen, entwickelten wir ein Tiermodell, welches auf Immunofärbungen mit pERK

basiert. Nach Wassertrinken beobachteten wir einen Anstieg an pERK in Neuronen, die hepatische Blutgefäße innervieren, was auf eine Beteiligung der Leber an peripherer Osmorezeption hindeutet. Weiterhin wurde die Osmosensitivität von DRG Neuronen des cervikalen und lumbaren Bereichs des Rückenmarks, sowie des Thoraxbereiches mittels Ca^{2+}-Imaging und der Patch-Clamp Methode untersucht. Wir fanden einen signifikant größeren Anteil an osmosensitiven Neuronen im Thoraxbereich im Vergleich zu anderen Bereichen des Rückenmarks. Mittels hepatischer Injektion eines retrograden Tracers konnten wir die Leber-innervierende Population an Neuronen des Thoraxbereiches markieren und zeigen, dass ein erheblicher Anteil dieser Poppulation osmosensitive ist, wodurch die Beteiligung der Leber an peripherer Osmoreception nachgewiesen werden konnte. Durch weitere Patch-Clamp Experimente wurde ausserdem gezeigt, dass nicht Neuronen der Nodose Ganglionen, sondern des Thoraxbereiches osmotische Stimuli in der Leber detektieren.

Ein großer Teil dieser Arbeit beschäftigte sich mit Untersuchungen von TRPV4 -/- Mäusen. Dabei beobachteten wir, dass die Deletion des TRPV4 Genes dazu führt, dass die Menge an pERK in hepatischen Afferenzen nach Wassertrinken nicht mehr ansteigt. Desweiteren war der Anteil an osmosensitiven Neuronen des Thoraxbereiches von TRPV4 -/- Tieren deutlich verringert, wie wir durch Ca^{2+} Imaging und Patch-Clamp Studien herausfanden. Unsere Ergebnisse deuten darauf hin, dass TRPV4 eine wesentliche Rolle bei der peripheren Osmorezeption spielt.

6 References

Adachi, A. (1984). "Thermosensitive and osmoreceptive afferent fibers in the hepatic branch of the vagus nerve." J Auton Nerv Syst **10**(3-4): 269-73.

Adachi, A., A. Niijima, et al. (1976). "An hepatic osmoreceptor mechanism in the rat: electrophysiological and behavioral studies." Am J Physiol **231**(4): 1043-9.

Alessandri-Haber, N., O. A. Dina, et al. (2006). "A transient receptor potential vanilloid 4-dependent mechanism of hyperalgesia is engaged by concerted action of inflammatory mediators." J Neurosci **26**(14): 3864-74.

Alessandri-Haber, N., E. Joseph, et al. (2005). "TRPV4 mediates pain-related behavior induced by mild hypertonic stimuli in the presence of inflammatory mediator." Pain **118**(1-2): 70-9.

Andersen, L. J., J. L. Andersen, et al. (2002). "Natriuresis induced by mild hypernatremia in humans." Am J Physiol Regul Integr Comp Physiol **282**(6): R1754-61.

Andersson, B. (1971). "Thirst--and brain control of water balance." Am Sci **59**(4): 408-15.

Andersson, B. (1978). "Regulation of water intake." Physiol Rev **58**(3): 582.

Averill, S., S. B. McMahon, et al. (1995). "Immunocytochemical localization of trkA receptors in chemically identified subgroups of adult rat sensory neurons." Eur J Neurosci **7**(7): 1484-94.

Ayus, J. C., J. Varon, et al. (2000). "Hyponatremia, cerebral edema, and noncardiogenic pulmonary edema in marathon runners." Ann Intern Med **132**(9): 711-4.

Baertschi, A. J. and R. A. Pence (1995). "Gut-brain signaling of water absorption inhibits vasopressin in rats." Am J Physiol **268**(1 Pt 2): R236-47.

Baertschi, A. J. and P. G. Vallet (1981). "Osmosensitivity of the hepatic portal vein area and vasopressin release in rats." J Physiol **315**: 217-30.

Barja, F. and R. Mathison (1984). "Sensory innervation of the rat portal vein and the hepatic artery." J Auton Nerv Syst **10**(2): 117-25.

Bennett, D. L., G. J. Michael, et al. (1998). "A distinct subgroup of small DRG cells express GDNF receptor components and GDNF is protective for these neurons after nerve injury." J Neurosci **18**(8): 3059-72.

Berthoud, H. R. (2004). "Anatomy and function of sensory hepatic nerves." Anat Rec A Discov Mol Cell Evol Biol **280**(1): 827-35.

Berthoud, H. R., M. Kressel, et al. (1992). "An anterograde tracing study of the vagal innervation of rat liver, portal vein and biliary system." Anat Embryol (Berl) **186**(5): 431-42.

Bicknell, R. J. (1988). "Optimizing release from peptide hormone secretory nerve terminals." J Exp Biol **139**: 51-65.

Birder, L. A., Y. Nakamura, et al. (2002). "Altered urinary bladder function in mice lacking the vanilloid receptor TRPV1." Nat Neurosci **5**(9): 856-60.
Blaine, E. H., D. A. Denton, et al. (1975). "A central osmosensitive receptor for renal sodium excretion." J Physiol **244**(2): 497-509.
Blair-West, J. R., A. P. Gibson, et al. (1985). "Acute reduction of plasma vasopressin levels by rehydration in sheep." Am J Physiol **248**(1 Pt 2): R68-71.
Boschmann, M., J. Steiniger, et al. (2003). "Water-induced thermogenesis." J Clin Endocrinol Metab **88**(12): 6015-9.
Bourque, C. W. (2008). "Central mechanisms of osmosensation and systemic osmoregulation." Nat Rev Neurosci **9**(7): 519-31.
Bourque, C. W. and S. H. Oliet (1997). "Osmoreceptors in the central nervous system." Annu Rev Physiol **59**: 601-19.
Bourque, C. W., S. H. Oliet, et al. (1994). "Osmoreceptors, osmoreception, and osmoregulation." Front Neuroendocrinol **15**(3): 231-74.
Brierley, S. M., A. J. Page, et al. (2008). "Selective role for TRPV4 ion channels in visceral sensory pathways." Gastroenterology **134**(7): 2059-69.
Brimble, M. J. and R. E. Dyball (1977). "Characterization of the responses of oxytocin- and vasopressin-secreting neurones in the supraoptic nucleus to osmotic stimulation." J Physiol **271**(1): 253-71.
Buggy, J., W. E. Hoffman, et al. (1979). "Osmosensitivity of rat third ventricle and interactions with angiotensin." Am J Physiol **236**(1): R75-82.
Buggy, J. and A. K. Jonhson (1977). "Preoptic-hypothalamic periventricular lesions: thirst deficits and hypernatremia." Am J Physiol **233**(1): R44-52.
Bykowski, M. R., J. C. Smith, et al. (2007). "Regulation of NaCl solution intake and gastric emptying in adrenalectomized rats." Physiol Behav **92**(5): 781-9.
Carlson, S. H., A. Beitz, et al. (1997). "Intragastric hypertonic saline increases vasopressin and central Fos immunoreactivity in conscious rats." Am J Physiol **272**(3 Pt 2): R750-8.
Caterina, M. J., M. A. Schumacher, et al. (1997). "The capsaicin receptor: a heat-activated ion channel in the pain pathway." Nature **389**(6653): 816-24.
Cenac, N., C. Altier, et al. (2008). "Transient receptor potential vanilloid-4 has a major role in visceral hypersensitivity symptoms." Gastroenterology **135**(3): 937-46, 946 e1-2.
Chen, Z., T. B. Gibson, et al. (2001). "MAP kinases." Chem Rev **101**(8): 2449-76.
Cheng, W., F. Yang, et al. (2007). "Thermosensitive TRPV channel subunits coassemble into heteromeric channels with intermediate conductance and gating properties." J Gen Physiol **129**(3): 191-207.
Choi-Kwon, S. and A. J. Baertschi (1991). "Splanchnic osmosensation and vasopressin: mechanisms and neural pathways." Am J Physiol **261**(1 Pt 1): E18-25.
Chwalbinska-Moneta, J. (1979). "Role of hepatic portal osmoreception in the control of ADH release." Am J Physiol **236**(6): E603-9.

Ciura, S. and C. W. Bourque (2006). "Transient receptor potential vanilloid 1 is required for intrinsic osmoreception in organum vasculosum lamina terminalis neurons and for normal thirst responses to systemic hyperosmolality." J Neurosci **26**(35): 9069-75.
Clapham, D. E., D. Julius, et al. (2005). "International Union of Pharmacology. XLIX. Nomenclature and structure-function relationships of transient receptor potential channels." Pharmacol Rev **57**(4): 427-50.
Claybaugh, J. R., A. K. Sato, et al. (2000). "Effects of time of day, gender, and menstrual cycle phase on the human response to a water load." Am J Physiol Regul Integr Comp Physiol **279**(3): R966-73.
Colbert, H. A., T. L. Smith, et al. (1997). "OSM-9, a novel protein with structural similarity to channels, is required for olfaction, mechanosensation, and olfactory adaptation in Caenorhabditis elegans." J Neurosci **17**(21): 8259-69.
Cosens, D. J. and A. Manning (1969). "Abnormal electroretinogram from a Drosophila mutant." Nature **224**(5216): 285-7.
Cserr, H. F., M. DePasquale, et al. (1987). "Regulation of brain water and electrolytes during acute hyperosmolality in rats." Am J Physiol **253**(3 Pt 2): F522-9.
Damann, N., T. Voets, et al. (2008). "TRPs in our senses." Curr Biol **18**(18): R880-9.
Darrow, D. C. and H. Yannet (1935). "The Changes In The Distribution Of Body Water Accompanying Increase And Decrease In Extracellular Electrolyte." J Clin Invest **14**(2): 266-75.
Dietz, T. H., R. A. Byrne, et al. (1995). "Paracellular solute uptake by the freshwater zebra mussel Dreissena polymorpha." Am J Physiol **269**(2 Pt 2): R300-7.
Djouhri, L., L. Bleazard, et al. (1998). "Association of somatic action potential shape with sensory receptive properties in guinea-pig dorsal root ganglion neurones." J Physiol **513 (Pt 3)**: 857-72.
Dunn, F. L., T. J. Brennan, et al. (1973). "The role of blood osmolality and volume in regulating vasopressin secretion in the rat." J Clin Invest **52**(12): 3212-9.
Egan, G., T. Silk, et al. (2003). "Neural correlates of the emergence of consciousness of thirst." Proc Natl Acad Sci U S A **100**(25): 15241-6.
Emmeluth, C., K. L. Goetz, et al. (1996). "Natriuresis caused by increased carotid Na+ concentration after renal denervation." Am J Physiol **270**(3 Pt 2): F510-7.
Fregly, M. J. (1967). "Effect of exposure to cold on evaporative loss from rats." Am J Physiol **213**(4): 1003-8.
Geelen, G., L. C. Keil, et al. (1984). "Inhibition of plasma vasopressin after drinking in dehydrated humans." Am J Physiol **247**(6 Pt 2): R968-71.
Gilman, A. (1937). "The relation between blood osmotic pressure, fluid distribution, and voluntary water intake." American Journal of Physiology **120**: 323-328.
Gilman, A. and L. Goodman (1937). "The secretory response of the posterior pituitary to the need for water conservation." J Physiol **90**(2): 113-24.

Greenleaf, J. E. (1982). "Dehydration-induced drinking in humans." Fed Proc **41**(9): 2509-14.
Gullans, S. R. and J. G. Verbalis (1993). "Control of brain volume during hyperosmolar and hypoosmolar conditions." Annu Rev Med **44**: 289-301.
Gutman, M. B., J. Ciriello, et al. (1988). "Effects of plasma angiotensin II and hypernatremia on subfornical organ neurons." Am J Physiol **254**(5 Pt 2): R746-54.
Haberich, F. J. (1968). "Osmoreception in the portal circulation." Fed Proc **27**(5): 1137-41.
Haberich, F. J. (1968). "[Significance of the portal circulation and the liver in regulation of the water-electrolyte balance]." Hippokrates **39**(21): 793-805.
Honda, K., H. Negoro, et al. (1990). "The osmoreceptor complex in the rat: evidence for interactions between the supraoptic and other diencephalic nuclei." J Physiol **431**: 225-41.
Huang, W., S. L. Lee, et al. (1996). "Dehydration natriuresis in male rats is mediated by oxytocin." Am J Physiol **270**(2 Pt 2): R427-33.
Huang, W., A. F. Sved, et al. (2000). "Water ingestion provides an early signal inhibiting osmotically stimulated vasopressin secretion in rats." Am J Physiol Regul Integr Comp Physiol **279**(3): R756-60.
Jewell, P. A. and E. B. Verney (1957). "An experimental attempt to determine the site of the neurohypophyseal osmoreceptors in the dog." Philos. Trans. R. Soc. London Ser. B **240**: 197-324.
Jordan, J., J. R. Shannon, et al. (2000). "The pressor response to water drinking in humans: a sympathetic reflex?" Circulation **101**(5): 504-9.
Jordan, J., J. R. Shannon, et al. (1999). "A potent pressor response elicited by drinking water." Lancet **353**(9154): 723.
Kleeman, C. R., H. Davson, et al. (1962). "Urea transport in the central nervous system." Am J Physiol **203**: 739-47.
Koerber, H. R., R. E. Druzinsky, et al. (1988). "Properties of somata of spinal dorsal root ganglion cells differ according to peripheral receptor innervated." J Neurophysiol **60**(5): 1584-96.
Lewin, G. R. and R. Moshourab (2004). "Mechanosensation and pain." J Neurobiol **61**(1): 30-44.
Lewis, T. S., P. S. Shapiro, et al. (1998). "Signal transduction through MAP kinase cascades." Adv Cancer Res **74**: 49-139.
Liedtke, W., Y. Choe, et al. (2000). "Vanilloid receptor-related osmotically activated channel (VR-OAC), a candidate vertebrate osmoreceptor." Cell **103**(3): 525-35.
Liedtke, W. and J. M. Friedman (2003). "Abnormal osmotic regulation in trpv4-/- mice." Proc Natl Acad Sci U S A **100**(23): 13698-703.
Liedtke, W., D. M. Tobin, et al. (2003). "Mammalian TRPV4 (VR-OAC) directs behavioral responses to osmotic and mechanical stimuli in Caenorhabditis elegans." Proc Natl Acad Sci U S A **100 Suppl 2**: 14531-6.
Lipp, A., J. Tank, et al. (2005). "Osmosensitive mechanisms contribute to the water drinking-induced pressor response in humans." Neurology **65**(6): 905-7.

Machino, T. and T. Yoshizawa (2006). "Brain shrinkage due to acute hypernatremia." Neurology **67**(5): 880.
Magni, F. and C. Carobi (1983). "The afferent and preganglionic parasympathetic innervation of the rat liver, demonstrated by the retrograde transport of horseradish peroxidase." J Auton Nerv Syst **8**(3): 237-60.
Maresh, C. M., J. A. Herrera-Soto, et al. (2001). "Perceptual responses in the heat after brief intravenous versus oral rehydration." Med Sci Sports Exerc **33**(6): 1039-45.
McKinley, M. J., D. A. Denton, et al. (1982). "Osmoregulatory thirst in sheep is disrupted by ablation of the anterior wall of the optic recess." Brain Res **236**(1): 210-5.
McKinley, M. J., D. A. Denton, et al. (1978). "Sensors for antidiuresis and thirst--osmoreceptors or CSF sodium detectors?" Brain Res **141**(1): 89-103.
McKinley, M. J., B. Lichardus, et al. (1992). "Periventricular lesions block natriuresis to hypertonic but not isotonic NaCl loads." Am J Physiol **262**(1 Pt 2): F98-107.
Mei, N. and L. Garnier (1986). "Osmosensitive vagal receptors in the small intestine of the cat." J Auton Nerv Syst **16**(3): 159-70.
Minke, B. (1977). "Drosophila mutant with a transducer defect." Biophys Struct Mech **3**(1): 59-64.
Mizuno, A., N. Matsumoto, et al. (2003). "Impaired osmotic sensation in mice lacking TRPV4." Am J Physiol Cell Physiol **285**(1): C96-101.
Molliver, D. C., D. E. Wright, et al. (1997). "IB4-binding DRG neurons switch from NGF to GDNF dependence in early postnatal life." Neuron **19**(4): 849-61.
Montell, C. (2005). "The TRP superfamily of cation channels." Sci STKE **2005**(272): re3.
Montell, C., K. Jones, et al. (1985). "Rescue of the Drosophila phototransduction mutation trp by germline transformation." Science **230**(4729): 1040-3.
Montell, C. and G. M. Rubin (1989). "Molecular characterization of the Drosophila trp locus: a putative integral membrane protein required for phototransduction." Neuron **2**(4): 1313-23.
Muraki, K., Y. Iwata, et al. (2003). "TRPV2 is a component of osmotically sensitive cation channels in murine aortic myocytes." Circ Res **93**(9): 829-38.
Nilius, B. (2007). "TRP channels in disease." Biochim Biophys Acta **1772**(8): 805-12.
Oliet, S. H. and C. W. Bourque (1993). "Mechanosensitive channels transduce osmosensitivity in supraoptic neurons." Nature **364**(6435): 341-3.
Raj, S. R., I. Biaggioni, et al. (2006). "Sodium paradoxically reduces the gastropressor response in patients with orthostatic hypotension." Hypertension **48**(2): 329-34.
Reiter, B., R. Kraft, et al. (2006). "TRPV4-mediated regulation of epithelial permeability." Faseb J **20**(11): 1802-12.

Richard, D. and C. W. Bourque (1994). "Osmotic activation of neurons dissociated from the OVLT and median preoptic nucleus (MnPO)." Soc. Neurosci. Abstr.
Robertson, G. L., R. L. Shelton, et al. (1976). "The osmoregulation of vasopressin." Kidney Int **10**(1): 25-37.
Roux, P. P. and J. Blenis (2004). "ERK and p38 MAPK-activated protein kinases: a family of protein kinases with diverse biological functions." Microbiol Mol Biol Rev **68**(2): 320-44.
Rutter, A. R., Q. P. Ma, et al. (2005). "Heteromerization and colocalization of TrpV1 and TrpV2 in mammalian cell lines and rat dorsal root ganglia." Neuroreport **16**(16): 1735-9.
Schroeder, C., V. E. Bush, et al. (2002). "Water drinking acutely improves orthostatic tolerance in healthy subjects." Circulation **106**(22): 2806-11.
Scott, E. M., J. P. Greenwood, et al. (2001). "Water ingestion increases sympathetic vasoconstrictor discharge in normal human subjects." Clin Sci (Lond) **100**(3): 335-42.
Sharif-Naeini, R., S. Ciura, et al. (2008). "Contribution of TRPV channels to osmosensory transduction, thirst, and vasopressin release." Kidney Int **73**(7): 811-5.
Sharif Naeini, R., M. F. Witty, et al. (2006). "An N-terminal variant of Trpv1 channel is required for osmosensory transduction." Nat Neurosci **9**(1): 93-8.
Silverman, A. J. and E. A. Zimmerman (1983). "Magnocellular neurosecretory system." Annu Rev Neurosci **6**: 357-80.
Silverman, J. D. and L. Kruger (1990). "Selective neuronal glycoconjugate expression in sensory and autonomic ganglia: relation of lectin reactivity to peptide and enzyme markers." J Neurocytol **19**(5): 789-801.
Snider, W. D. and S. B. McMahon (1998). "Tackling pain at the source: new ideas about nociceptors." Neuron **20**(4): 629-32.
Sofroniew, M. V., A. Weindl, et al. (1979). "The distribution of vasopressin-, oxytocin-, and neurophysin-producing neurons in the guinea pig brain. I. The classical hypothalamo-neurophypophyseal system." Cell Tissue Res **196**(3): 367-84.
Somero, G. N. (1986). "Protons, osmolytes, and fitness of internal milieu for protein function." Am J Physiol **251**(2 Pt 2): R197-213.
Steenbergen, C., M. L. Hill, et al. (1985). "Volume regulation and plasma membrane injury in aerobic, anaerobic, and ischemic myocardium in vitro. Effects of osmotic cell swelling on plasma membrane integrity." Circ Res **57**(6): 864-75.
Strange, K. (2004). "Cellular volume homeostasis." Adv Physiol Educ **28**(1-4): 155-9.
Stricker, E. M. and M. L. Hoffmann (2007). "Presystemic signals in the control of thirst, salt appetite, and vasopressin secretion." Physiol Behav **91**(4): 404-12.
Stricker, E. M. and J. G. Verbalis (1987). "Central inhibitory control of sodium appetite in rats: correlation with pituitary oxytocin secretion." Behav Neurosci **101**(4): 560-7.

Strotmann, R., C. Harteneck, et al. (2000). "OTRPC4, a nonselective cation channel that confers sensitivity to extracellular osmolarity." Nat Cell Biol **2**(10): 695-702.
Stucky, C. L. and G. R. Lewin (1999). "Isolectin B(4)-positive and -negative nociceptors are functionally distinct." J Neurosci **19**(15): 6497-505.
Suzuki, M., A. Mizuno, et al. (2003). "Impaired pressure sensation in mice lacking TRPV4." J Biol Chem **278**(25): 22664-8.
Swaab, D. F., C. W. Pool, et al. (1975). "Immunofluorescence of vasopressin and oxytocin in the rat hypothalamo-neurohypophypopseal system." J Neural Transm **36**(3-4): 195-215.
Tank, J., C. Schroeder, et al. (2003). "Pressor effect of water drinking in tetraplegic patients may be a spinal reflex." Hypertension **41**(6): 1234-9.
Thrasher, T. N., C. J. Brown, et al. (1980). "Thirst and vasopressin release in the dog: an osmoreceptor or sodium receptor mechanism?" Am J Physiol **238**(5): R333-9.
Thrasher, T. N., L. C. Keil, et al. (1982). "Lesions of the organum vasculosum of the lamina terminalis (OVLT) attenuate osmotically-induced drinking and vasopressin secretion in the dog." Endocrinology **110**(5): 1837-9.
Vallet, P. G. and A. J. Baertschi (1982). "Spinal afferents for peripheral osmoreceptors in the rat." Brain Res **239**(1): 271-4.
Verbalis, J. G. (2003). "Disorders of body water homeostasis." Best Pract Res Clin Endocrinol Metab **17**(4): 471-503.
Verbalis, J. G., E. F. Baldwin, et al. (1986). "Osmotic regulation of plasma vasopressin and oxytocin after sustained hyponatremia." Am J Physiol **250**(3 Pt 2): R444-51.
Verney, E. B. (1947). "The antidiuretic hormone and the factors which determine its release." Proc R Soc Lond B Biol Sci **135**(878): 25-106.
Viana, F., E. de la Pena, et al. (2001). "Swelling-activated calcium signalling in cultured mouse primary sensory neurons." Eur J Neurosci **13**(4): 722-34.
Watanabe, H., J. Vriens, et al. (2003). "Anandamide and arachidonic acid use epoxyeicosatrienoic acids to activate TRPV4 channels." Nature **424**(6947): 434-8.
Zhang, Z. and C. W. Bourque (2003). "Osmometry in osmosensory neurons." Nat Neurosci **6**(10): 1021-2.
Zhang, Z., A. N. Kindrat, et al. (2007). "Actin filaments mediate mechanical gating during osmosensory transduction in rat supraoptic nucleus neurons." J Neurosci **27**(15): 4008-13.